

Review

Photocatalytic Inactivation as a Method of Elimination of *E. coli* from Drinking Water

Timothy O. Ajiboye^{1,2} , Stephen O. Babalola³ and Damian C. Onwudiwe^{1,2,*} 

¹ Material Science Innovation and Modelling (MaSIM) Research Focus Area, Faculty of Natural and Agricultural Science, North-West University (Mafikeng Campus), Private Bag X2046, Mmabatho 2735, South Africa; 32480342@student.g.nwu.ac.za

² Department of Chemistry, Faculty of Natural and Agricultural Science, North-West University (Mafikeng Campus), Private Bag X2046, Mmabatho 2735, South Africa

³ Department of Biology/Microbiology/Biotechnology, Alex Ekwueme Federal University, Ndufu-Alike Ikwo, Ebonyi State 84001, Nigeria; Stephen.babalola@funai.edu.ng

* Correspondence: Damian.Onwudiwe@nwu.ac.za; Tel.: +27-18-389-2545; Fax: +27-18-389-2420

Abstract: The presence of microorganisms, specifically the *Escherichia coli*, in drinking water is of global concern. This is mainly due to the health implications of these pathogens. Several conventional methods have been developed for their removal; however, this pathogen is still found in most drinking water. In the continuous quest for a more effective removal approach, photocatalysis has been considered as an alternative method for the elimination of pathogens including *E. coli* from water. Photocatalysis has many advantages compared to the conventional methods. It offers the advantage of non-toxicity and utilizes the energy from sunlight, thereby making it a completely green route. Since most photocatalysts could only be active in the ultraviolet region of the solar spectrum, which is less than 5% of the entire spectrum, the challenge associated with photocatalysis is the design of a system for the effective harvest and complete utilization of the solar energy for the photocatalytic process. In this review, different photocatalysts for effective inactivation of *E. coli* and the mechanism involved in the process were reviewed. Various strategies that have been adopted in order to modulate the band gap energy of these photocatalysts have been explored. In addition, different methods of estimating and detecting *E. coli* in drinking water were presented. Furthermore, different photocatalytic reactor designs for photocatalytic inactivation of *E. coli* were examined. Finally, the kinetics of *E. coli* inactivation was discussed.

Keywords: photocatalysis; water treatment; *Escherichia coli*; bacteria inactivation



Citation: Ajiboye, T.O.; Babalola, S.O.; Onwudiwe, D.C. Photocatalytic Inactivation as a Method of Elimination of *E. coli* from Drinking Water. *Appl. Sci.* **2021**, *11*, 1313. <https://doi.org/10.3390/app11031313>

Received: 29 November 2020

Accepted: 2 January 2021

Published: 1 February 2021

Publisher's Note: MDPI stays neutral with regard to jurisdictional claims in published maps and institutional affiliations.



Copyright: © 2021 by the authors. Licensee MDPI, Basel, Switzerland. This article is an open access article distributed under the terms and conditions of the Creative Commons Attribution (CC BY) license (<https://creativecommons.org/licenses/by/4.0/>).

1. Introduction

Water is an essential natural resource and, perhaps, the greatest need of humanity for health, wellbeing, development, and sustenance of life [1–3]. Its availability and accessibility plays an important role in food production, poverty reduction, social welfare and economic development [1]. Water has so many functions in the body, such as the maintenance of the normal volume and consistency of blood and lymph, modulation of moisture content of internal organs of the body, removal of poisons or toxins from the body through urine, sweat and breathing, the regulation of body temperature. It is also essential for the regulation of the normal structure and functions of the skin [1]. Unfortunately, about 20% of the world's population has no access to clean drinking water, a problem which is further complicated by the increasing world population [4]. According to the World Health Organization report of 2015, more than 2.6 billion people lack safe drinking water, leading to the death of about 3.4 million people from various water related diseases each year. Of these deaths, 1.4 million were reported to be children [5,6].

The exposure to preventable health risks has been attributed to the absence, inadequacy, or inappropriately managed water and sanitation services. Some of the health risks

and diseases associated with the lack or insufficient clean water supply include hepatitis, cholera, typhus, polio, tuberculosis, diphtheria and diarrhea. These have become a problem of global concern [7,8]. Diarrhea is largely preventable, but it remains the most widely known disease linked to contaminated food and water. About 829,000 yearly deaths are attributed to diarrhea, and this is due to unsafe drinking-water, poor sanitation, and inadequate hand hygiene [7]. Although these water-related diseases are common in developing countries, they are also a challenging health concern in the developed world [3,6]. Thus, water quality control from water treatment plants continues to be an important global topic of public health concern in the water industry. Shortage of fresh and portable water supply is also combated through water recycling and reuse. However, this is also constrained due to the need to completely eliminate contaminants in waste water [9]. Hence, the decontamination of water from both chemical and microbial (biological) contaminants is a major problem that must be solved especially in developing nations of the world. Microbial contaminants are often considered a higher priority than chemical contaminants because the adverse health effects of microbial contaminants are immediate, while that of chemical contaminants are connected with long-term exposures [2]. Most biological agents that cause water borne diseases are transmitted to humans via sewage discharge into water sources [8].

In water treatment plants, a simple and reliable microbiological water quality control of drinking water is often required to assess and monitor the presence of these pathogens, especially the faecal coliforms [1,6]. These are a group of bacteria that emanate from the faecal droppings of livestock, wildlife and humans. *Escherichia coli* (*E. coli*) is the most abundant of this category, and it is often associated with the health risk of water [3,6]. There is a high possibility of the presence of other harmful viruses and bacteria of faecal origin when *E. coli* is present in water samples. Pathogenic microbes such as *Giardia*, *Cryptosporidium*, and *Shigella* may also be found in water samples where *E. coli* is present [3]. This is why *E. coli* is often used as an indicator organism or a benchmark for determining water purity and for the assessment of water samples containing faecal contaminants beyond acceptable levels [1,3,6,8]. Two key factors are responsible for the use of *E. coli* as the preferred indicator for the detection of faecal contamination in drinking water: firstly, some faecal coliforms are non faecal in origin; and, secondly, there are well-developed and improved testing methods for *E. coli* [1]. Consequently, *E. coli* is also used to evaluate the efficiency of water disinfection methods. If the water sample is free from *E. coli* after a disinfection process, it is concluded that the method is efficient and the water is free from faecal contamination—thus making it unnecessary to analyze the water sample for other pathogens [8,10–12].

Several conventional water disinfection methods such as chlorination, ozonation, radiation, advanced filtration, and the use of ultraviolet (UV) light have been used over the years [3,13]. Water decontamination by chlorination, for example, uses chlorine as a strong oxidant, and it is one of the important, most common, relatively simple, effective and inexpensive conventional ways to provide biologically potable water [3,4,10,13,14]. Unfortunately, conventional water purification technologies have several drawbacks, some of which include:

- Formation of Disinfection Byproducts (DBPs) and their consequent carcinogenicity: Chemical disinfection methods such as chlorination and ozonation could also lead to the formation of toxic and corrosive disinfection byproducts such as trihalomethanes (THM), chloroform, chlorite, and haloacetic acids. This is due to high amount of content of free residual chemicals after the disinfection process, and these compounds have been proven to be extremely carcinogenic [3,4,8,9,13,15,16].
- High operation and maintenance cost: Expensive chemicals or equipment are required for the operation and maintenance of many of these methods. For instance, water decontamination with ultraviolet light applies shortwave radiation (<280 nm) and is associated with increased energy utilization. This requires expensive equipment for the production [13,15,16].

- Antibiotic drug resistance: Microorganisms soon become resistant to some of these conventional methods with prolonged use, thereby making the method ineffective for water disinfection over time. Some biohazards are even naturally resistant to chlorination and UV treatments [9,16–18].
- Low disinfection efficiency: For example, chlorination is not able to eliminate all pathogens. This is due to its slow biodegradation kinetics [8,13].

Moreover, the conventional disinfection technologies are often met with implementation challenges. A high concentration of residual chemicals could cause an unpleasant taste and smell in the drinking water [13,16]. Ozonation, chlorination and other techniques have been used for removing these bacteria, but they usually produce toxic by-products and some of these byproducts may be mutagenic or carcinogenic [19,20]. In fact, disinfection with the help of UV radiation alone, which is considered as a good alternative due to the fact that the introduction of chemicals is not required, has now been discovered to be disadvantageous. This is because some bacteria are resistant to UV radiation since they regenerate after a few hours of irradiation [19,20]. Hence, there is a great need for alternative water disinfection technologies that could make up for the inherent limitations of the conventional water decontamination methods [3]. Recent studies have been focused on the development of an advanced antibacterial technology against microbial contaminants in water. Specifically, a more efficient method of inactivating bacteria such as *E. coli* is desirable.

Photocatalytic disinfection is considered as one of the innovative and promising options with high disinfection potential for water purification [13,15]. It is regarded as one of the most prominent advanced oxidation technologies (AOT) and has so many applications in water and air purification, viral and bacterial inactivation, and deodorization [16,21,22]. It has been an area of great interest in recent years, since it is applicable in many fields including environmental and energy related research areas [13]. Photocatalysis has so many advantages over the conventional water disinfection methods. Compared to the other conventional methods of inactivating *E. coli*, photocatalysis is better and promising because of its cost effectiveness [23]. Photocatalytic materials used for disinfection could be recycled, while the conventional chemical methods consume the chemical disinfectants [4]. Finally, the photocatalytic materials used are non-hazardous and environmentally friendly, yet are effective in the inactivation of pathogenic microorganisms in water [4,8].

1.1. The Structure of *Escherichia coli*

In 1885, Theodore Escherich discovered and described *Bacillus coli*. It was then renamed *Escherichia coli* after his name [1,24] *E. coli* is a diverse group of gram-negative bacteria commonly found in the environment. They are also a normal part of the lower intestinal tract microbiota of mammals including humans [1,24,25]. *E. coli* are typically rod-like in shape with about 2 micrometres (μm) length, a diameter of 0.5 μm and a cell volume of about 0.6–0.7 μm^3 [1,26]. They are non-sporulating and use mixed-acid anaerobic fermentation to produce carbon dioxide, ethanol, lactate, acetate, and succinate. Some strains of *E. coli* could grow at temperatures up to 49 °C, but the temperature for optimal growth is about 37 °C [1,26]. The cell wall of *E. coli* is made of a thick layer of protein and sugar that prevents the cell from bursting. The plasma membrane, made of lipids and proteins, regulates the movement of molecules in and out of the cell. The fimbriae help the *E. coli* to attach itself to surfaces, while ribosomes aid in the production of proteins [1]. The flagella are composed of proteins, giving cells the capability to move (Figure 1).

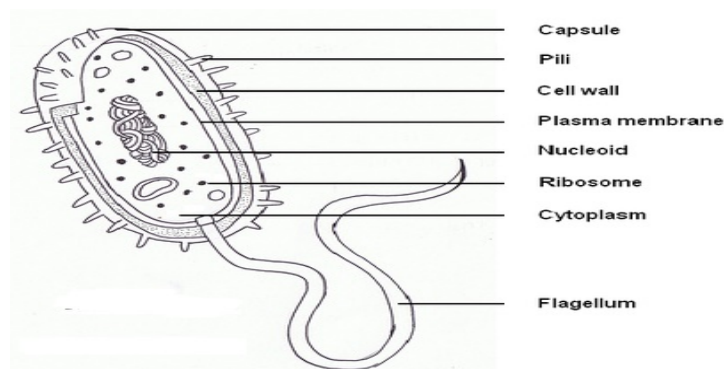


Figure 1. Structure of *Escherichia coli*. Reprinted from [24].

1.2. The Different Strains of *Escherichia coli*

E. coli is one of the most studied living organisms due to the enormous clinical and scientific interests in the organism. It has been used as the model organism for studies in a lot of biological research including studies in genetics, molecular biology, and evolution [25]. Depending on the strain, *E. coli* could either be harmful or harmless. Both the pathogenic and non-pathogenic *E. coli* behave ecologically and biochemically alike, making it difficult to detect the pathogenic ones among commensal *E. coli* [25,27]. Meanwhile, the harmful pathogenic strains are responsible for diarrheal and other diseases in humans and animals [27,28]. The pathogenic strains have virulence factors involved in their pathogenesis and are used to group them into various pathotypes or virotypes [28]. There are two broad groups of pathogenic strains of *E. coli* depending on the site of infection:

- Intestinal Pathogenic *E. coli* (IPEC): Most pathogenic strains of *E. coli* are Intestinal pathogenic *E. coli*. They are also known as Enteric *E. coli*, and are the group of *E. coli* that elicit their pathological effects and cause diseases in the gastrointestinal tract [1,28]. Examples of Intestinal pathogenic *E. coli* include enteropathogenic *E. coli* (EPEC), enterohaemorrhagic *E. coli* (EHEC), enterotoxigenic *E. coli* (ETEC), enteroaggregative *E. coli* (EAEC), enteroinvasive *E. coli* (EIEC) and diffusely adherent *E. coli* (DAEC).
- Extra-Intestinal Pathogenic *E. coli* (EXPEC): Any other group of *E. coli* that cause diseases or exert their pathogenic syndromes in systems other than gastrointestinal tract are known as Extra-intestinal pathogenic *E. coli* [28]. Some of the examples of Extra-intestinal pathogenic *E. coli* includes sepsis-causing *E. coli* (SEPEC), uropathogenic *E. coli* (UPEC) and neonatal meningitis-associated *E. coli* (NMEC). The genomes of several strains of both pathogenic and non-pathogenic *E. coli* have been completely sequenced, others are being sequenced while many other strains will be sequenced in the future as new strains emerge through the natural biological process of mutation [1,25,27,28]. However, this review is limited to three of the most common strains of *E. coli* including: the non-pathogenic commensal, K-12 strain; the enterohemorrhagic O157:H7 strain, and the uropathogenic CFT073 strain.

1.2.1. The Non-Pathogenic K-12 Strain

Virulence genes found in *E. coli* are responsible for their pathogenic effects. The K-12 strains of *E. coli* lack all known *E. coli* virulence genes and are therefore considered to be a safe, nonpathogenic bacterial strain [29]. The harmless strains produce vitamin K2 and prevent the invasion of pathogenic bacteria within the intestine as they are often part of the normal flora of the gut [1]. *E. coli* K-12 strains are rough and the O antigen, which is part of the lipopolysaccharide, is absent [29]. In gene cloning experiments, *Escherichia coli* K-12 strains are the most commonly used host strains because of the following advantages:

- Genetically, they are a well understood group of living organisms.
- They could be modified easily by many genetic methods, and

- They are grouped as biologically safe vehicles for the propagation of many efficient gene cloning and expression vectors.

1.2.2. The Enterohaemorrhagic O157:H7 Strain

After the outbreak in 1982, *E. coli* O157:H7 became the most widely known enterohaemorrhagic *E. coli* (EHEC) strain [26]. Shiga toxin production, a characteristic feature of the pathogenesis of bloody diarrhea, was reported in Hemorrhagic Colitis outbreak caused by *E. coli* O157:H7 strain in the United States [26,28,30]. The ability to produce Shiga toxins is the common characteristic of all EHEC, and they are often referred to as Shiga toxin-producing *E. coli* (STEC) [26]. *E. coli* O157:H7 has been implicated in the death of the elderly, the very young, and the immunocompromised including serious food poisoning leading to product recalls [1]. Its pathogenicity coupled with its ability to survive environmental stress make it a powerful threat to public health efforts. It is resistant to commonly used methods for controlling bacteria such as boiling. The conventional means of isolating other *E. coli* are not effective in the isolation and identification of enterohaemorrhagic *E. coli* O157:H7 because it has some biochemical differences from most other *E. coli* strains [1,26,28,30]. For example,

- Ninety percent of other strains of *E. coli* cannot ferment sorbitol but O157:H7 strain can ferment it [1,26,28,30].
- It does not produce functional β -glucuronidase, whereas most of the other *E. coli* strains are positive for this test [1,26,28,30].
- Unlike the other 60% non-sorbitol fermenting *E. coli*, the O157:H7 strains will not ferment rhamnose on nutrient agar [1].

Therefore, special techniques such as DNA probes and polymerase chain reaction (PCR), ELISA procedure utilizing the monoclonal antibody (4E8C12) are used in the isolation of *E. coli* O157:H7 [1].

1.2.3. The Uropathogenic CFT073 Strain

About seventy to ninety percent of the estimated 150 million community acquired urinary tract infections are caused by the uropathogenic *E. coli* [31]. In the United States, 7 million cases of acute cystitis and 250,000 cases of pyelonephritis are reported annually, 70–90% of which are also caused by uropathogenic *E. coli* [31]. A lot of genes that code for fimbrial adhesins, phase-switch recombinases, autotransporter and iron sequestration systems are found in the genome of the uropathogenic *E. coli* CFT073 strain. These features predispose the strain to colonize the urinary tracts and elicit its pathological effects [32].

2. Mechanism of the Photocatalytic Inactivation of *E. coli*

Several studies have already discussed the mechanism of photocatalysis. Hence, only the summary is given in this review [33–36]. Photocatalysis is easy to implement as it essentially involves the use of a light source and a photocatalyst. An interaction between light and the semiconductor solid catalyst results in the absorption of light with energy equal to or greater than the band gap energy of the semiconductor photocatalyst. This leads to the excitation of electron(s) from the lower energy level, the valence band (VB), to the higher energy level, the conduction band (CB). Generally, semiconductors consist of an electron filled valence band and an empty conduction band [37]. The migration of electrons from the occupied VB leaves positively charged holes on the VB (electron vacancy). It is possible for both the electrons generated and the holes to recombine, which is not desirable because their combination will lead to the loss of energy informing of heat energy. The second possibility is the production of hydroxyl radicals as a result of the interaction of holes with water and superoxides are formed as a result of the interaction of the generated electron with oxygen [34,38] as shown in Figure 2. These photogenerated highly reactive species (ROS) or free radicals (such as hydroxyl radicals (OH \cdot) and superoxide (O $^{2-}$)) are capable of eliminating biological and chemical water contaminants [8,15,16]. The free radicals produced are highly effective antibacterial agents within aqueous environments.

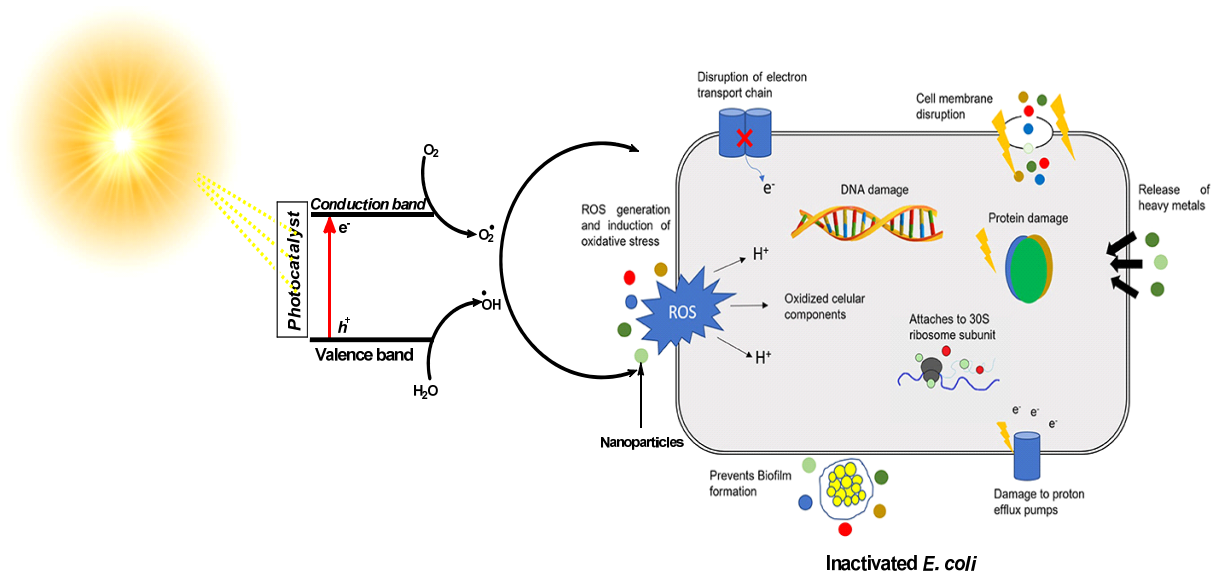


Figure 2. Mechanism of photocatalytic inactivation of *E. coli*.

Three common theories have been proposed for the mechanism of inactivation of bacteria. The first is the destruction of the DNA, the second is the inhibition of the respiratory activities as a result of the oxidation of coenzyme A by the photogenerated reactive species, which leads to their loss from the cells. The third mechanism is the destruction of the membranes by reactive species, thereby leading to cell content's leakage [35,39,40]. Irrespective of the mechanism, the inactivation is affected by the photogenerated holes, electrons, and the reactive oxygen species (such as hydroxyl radicals, peroxy radicals and hydroperoxyl radicals) generated during the mechanism of photocatalysis.

As the *E. coli* inactivation proceeds, the shape of *E. coli* cells begins to get disfigured and the shape becomes different from the original shape before the inactivation process. This is followed with the rupturing of the cell wall, which permits the reactive species to permeate the cell and the size of the remaining part of the cell decreases noticeably [41]. The inorganic species used to monitor the destruction is potassium ion, since it is responsible for regulating polysomes and proteins. Rupturing of cell membrane leads to the leaking of potassium ions. The concentration of potassium ion has been discovered to increase with an increase in the time of photocatalytic inactivation [9,41].

3. Inactivation Process by Photocatalysts

Several photocatalysts have been used to inactivate *E. coli*, and they include metal oxides, sulphides, halides, phosphide or other metal free photocatalysts. The type of light source used along with these photocatalysts depends on the band gap energy of the photocatalysts used [42]. These photocatalysts are not only photoactive, but they are non-toxic, of moderate band gap and inert, which are the desirable properties of the photocatalyst [33]. The redox potential of both the valence band and conduction band of different photocatalysts at neutral pH is shown in Figure 3.

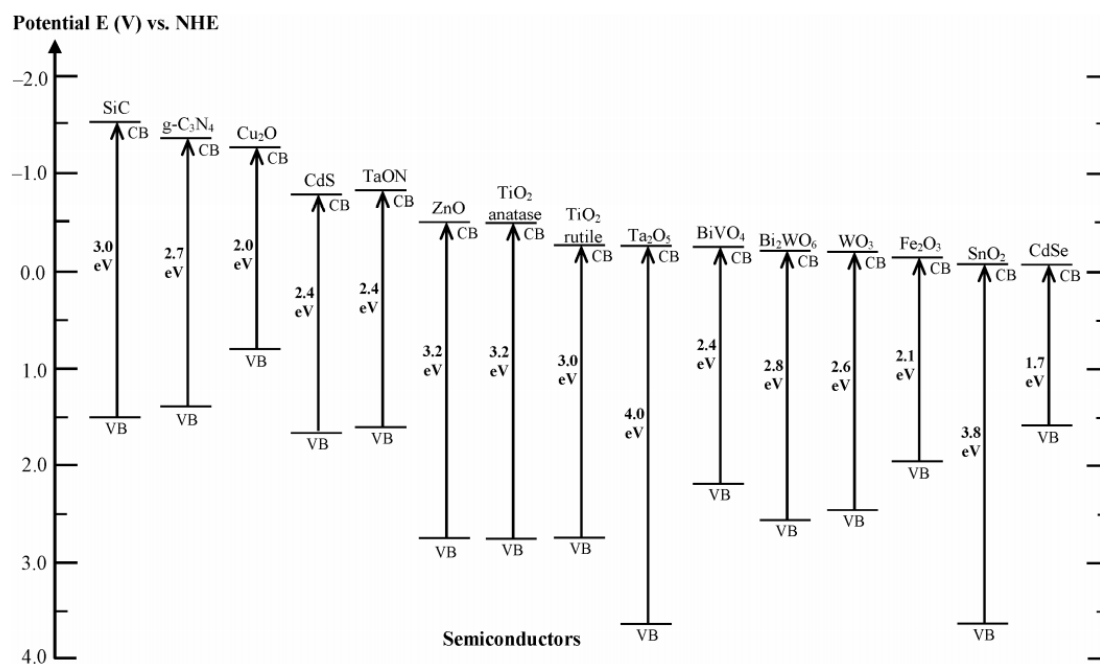


Figure 3. Redox potential and band gap energies of some selected semiconductor photocatalysts at pH 7. Reprinted with permission from [43], Copyright (2016) American Chemical Society.

The different compounds that have been utilized as semiconductor photocatalysts in the inactivation of *E. coli* will be highlighted and their specific properties discussed.

3.1. Metal Oxides as Photocatalysts for the Inactivation of *E. coli*

Metal oxides such as TiO₂, ZnO, ZrO₂, CeO₂, Fe₂O₃, SnO₂ and WO₃ have photocatalytic properties and have been reported in different studies [8,15,44–48]. The photocatalytic properties of some of these metal oxides have been harnessed for the conversion of solar energy to chemical energy in order to oxidize or reduce materials, degrade pollutants and inactivate pathogens [13]. Nanocomposite made from two oxides (zinc oxide and silver oxide) has been used to inactivate *E. coli* under both visible and ultraviolet light radiation. Despite pure zinc oxide being reported to be effective against bacteria [49], its photocatalytic activities were lower than that of the nanocomposite made from zinc oxide and silver oxide [50]. In a bid to reducing the time needed for the inactivation of bacteria, zinc oxide nanoarrays were fabricated and used to inactivate 97.5% of *E. coli* within 60 s under ultraviolet light. However, after several cycles of use, the time taken for inactivation to take place was 600 s under similar condition [51]. Oxides of copper nanoparticles derived from citrus has been used as light-sensitive catalysts for decontaminating wastewater containing *E. coli* [52]. Magnesium oxide nanoparticles obtained via green synthesis from plant biomass was also used to inhibit *E. coli* [53]. The synthesis of magnesium oxide from plant biomass is advantageous because it is not poisonous, is environmentally sustainable and cheaply available [54,55]. In addition, the biomass contains stabilizing and reducing agents such as phenolic compounds, natural acids, alkaloids, and terpenoids, which aid the formation of the nanoparticles of metal oxides [54,55]. The inactivation of 60% of *Escherichia coli* was achieved in the presence of light by using chitosan and sodium alginate functionalized by nanoparticles of ZnO and CuO. The functionalization led to the generation of more reactive oxygen species under light [56].

Titanium oxide is one of the earliest discovered catalysts and has remained the photocatalyst of choice due to its non-toxic nature, relative cheapness, good photocatalytic performance and high chemical stability [57]. It is an important nanomaterial with optical, catalytic and dielectric properties [58]. Titanium dioxide has attracted a considerable attention because of its wide and growing industrial applications in the production of

solar cells, fillers, pigments including catalyst supports and as photocatalysts [8,58]. It has three crystal forms, namely brookite, anatase and rutile. The anatase form induces maximum speed in the formation of free radicals [8]. Several studies have shown the potential of the TiO_2 catalyst in the successful and complete deactivation of microbial cells including cancerous cells, bacteria, viruses, fungi and algae under the irradiation of UV light source [58]. One of the numerous investigations that utilized titanium oxide as photocatalyst for inactivating *E. coli* was reported by Kikuchi et al. [59]. In the study, a transparent film of titanium oxide was used to inactivate *E. coli* in the presence of light. Hydrogen peroxide was introduced to increase the amount of reactive oxygen species that is present in the photocatalytic system. Despite the wide acceptance of titanium oxide as a good photocatalyst for inactivating bacteria, the limitation of titanium oxide photocatalyst is that it is only active in the ultraviolet (UV) region of the solar spectrum due to the wide band gap energy of 3.2 eV. This UV region accounts for less than 5% of the solar spectrum, which implies that pure titanium oxide under-utilizes the solar spectrum. Thus, different structural modifications of titanium oxide have been carried out to reduce the band gap energy of titanium oxide in order to absorb in the visible region of the solar spectrum, which accounts for the larger percentage of the spectrum. Titanium oxide also displays better bactericidal performance against *E. coli* when jointly doped with silver and nitrogen. The death of *E. coli* was ascribed to the disconfiguration of the cell and cell wall thinning through oxidative damage under visible light [60]. Ribeiro et al. [13], for example, reported that TiO_2 inactivated all *E. coli* cells within 60 min with UV light.

3.2. Metal Sulphides as Photocatalysts for the Inactivation of *E. coli*

Different types of sulphides have been reported for the inactivation of *E. coli*. For example, binary indium sulphide with band gap energy of 2.25 eV was used as the visible light sensitive photocatalyst for inactivating *E. coli*. Instead of hydroxyl radical causing the inactivation, hydrogen peroxide, peroxy radicals, holes and electrons were reported as the cause of inactivation as confirmed by the scavenger investigation. These reactive species caused 5 log inactivation of bacteria cell by destroying enzymes and DNA, which are cytoplasmic components of the bacteria after 180 min of visible light irradiation [61]. Zinc sulphide has also been used for *E. coli* inactivation. When the photocatalyst was exposed to UV light, 99% of *E. coli* was inactivated within 120 min [62]. Apart from the binary sulphides, ternary sulphides were also used for *E. coli* inactivation. Wang et al. [63] reported the use of ternary CdIn_2S_4 as a visible light-active photocatalyst. The ternary compound was found to be effective because it could be recycled via partition without losing its performance. This photocatalyst was able to inactivate 7 log of the bacteria within 180 min. The efficiency of the bacteria inactivation was also found to improve with increase in the photocatalyst loading. A novel nanocrystal ternary sulphide (Cu_2WS_4) was used to inactivate more than 99% (5 log) of Gram-negative *E. coli* in the presence of light. Further investigation into the mechanism of antibacterial inactivation of this ternary sulphide photocatalyst showed that it has the ability to selectively bound to bacteria. In addition, it has peroxidase and oxidase properties, which enhanced the generation of reactive oxygen species that are active against *E. coli* [64].

3.3. Metal Halides as Photocatalyst for the Inactivation of *E. coli*

One of the metal halides that has been extensively studied for the inactivation of *E. coli* is the silver halides. Silver iodide has been decorated on an organic framework made from 1,3,5-triformylphloroglucinol and 2,5-diaminopyridine precursors and was used for inactivating *E. coli*. The application of silver iodide as photocatalyst against bacteria was found to be a good option because of its stability after four consecutive runs without losing its photocatalytic performance [65]. To inactivate *E. coli*, silver iodide has also been used along with cerium oxide [66], copper ferrite [67], bismuth oxyiodide [68], zinc ferrite [69], bismuth stannate ($\text{Bi}_2\text{Sn}_2\text{O}_7$) [70] and bismuth vanadate [70]. Silver bromide has also been an active photocatalyst against *E. coli*. Yu et al. [70] utilized silver bromide decorated

on graphitic carbon nitride to inactivate the bacteria in the presence of visible light. The effectiveness of silver bromide was obvious because 4.8 log of the bacteria was inactivated in the presence of silver bromide unlike 4.2 log that was inactivated when pure graphitic carbon nitride was utilized without silver bromide. More than 99% of the *E. coli* was inactivated by silver bromide when it was used along with silver vanadate for bacteria inactivation in the presence of light in less than an hour [71]. In addition, the elimination of *E. coli* by using silver bromide assisted with bismuth oxybromide has been reported [72]. The photocatalytic efficiency of silver bromide was boosted when it was used along with graphitic carbon nitride for eliminating *E. coli* [73]. Krutyakov et al. also reported the use of nanocomposite photocatalysts made from silver chlorides for the inactivation of *E. coli*. The photocatalyst was stabilized by amphopolycarboxyglycinate, which is sodium-containing amphoteric surfactant [74].

3.4. Metal Phosphides as Photocatalysts for the Inactivation of *E. coli*

Relatively less attention has been given to the use of phosphides as a photocatalysts, but the use of zinc phosphide has been well investigated [75,76]. The large abundance of zinc and phosphorus in the earth crust and the possibility of fabricating different morphologies with band gap that is as low as 1.5 eV makes zinc phosphide one of the photocatalysts that could be considered for the inactivation of *E. coli* [77]. The major drawback for the utilization of zinc phosphide is that it has low stability in water [75,77]. One of the adopted strategies for the improvement of its stability is to functionalize it with organic molecules [76]. Vance et al. used this strategy to improve the stability of zinc phosphide nanowire and boron nitride was used for the functionalization. The functionalized zinc phosphide was used for inactivating *E. coli* with 5-log of the bacteria inactivated within 300 s under visible light irradiation [76]. However, the photocatalytic activities of the un-functionalized phosphide were found to be better than that of the functionalized phosphide.

3.5. Metal Free Photocatalysts for the Inactivation of *E. coli*

One of the metal-free materials that has been used for inactivating *E. coli* is three-dimensional reduced graphene oxide and graphene oxide under visible light irradiation. The inactivation rate was boosted by five times when the peroxymonosulphate was introduced as an activator [78]. The inactivation was carried out through non-radical and radical reaction pathways. Holes, hydroxyl radicals, hydroperoxyl radicals and peroxy radicals were found to be the active radicals against the bacteria as revealed by the scavenger investigations carried out by the non-toxic scavengers. These non-toxic scavengers were selected to prevent damages to bacteria cells so as to obtain accurate quenching effects [78]. Graphene oxide quantum dots were also effective against *E. coli*, but when it was functionalized with nanorods and nanoflakes of zinc oxide, it was observed that these functionalized photocatalysts displayed better antibacterial efficiency than when ordinary graphene oxide quantum dots was utilized as photocatalysts [79]. Another metal-free photocatalyst that was used to inactivate *E. coli* is graphitic carbon nitride, and it was found to be effective against *E. coli*. However, the rate of inactivation was found to be better when graphitic carbon nitride was composited with molybdenum sulphide and bismuth oxide [80]. The graphitic carbon nitride was coupled with copper (I) oxide and used as photocatalyst under visible light to inactivate *E. coli*. Investigations by electron spin resonance and reactive species trapping revealed that the inactivation was effected by holes, hydroxyl radicals and peroxy radicals [81]. Huang et al. [82] used graphitic carbon nitride to inactivate *E. coli* k-12, and this was carried out in the presence of visible light irradiation. When the photocatalytic inactivation was carried out for 4 h, there was complete inactivation of the bacteria as confirmed using a bacteria regrowth test, which showed that there was no bacteria count after four days of incubation. It was also observed that, when graphitic carbon nitride was used in the dark, there was no effect on the bacteria. This showed that the inactivation was affected due to the presence of light. Graphitic carbon nitride nanosheet has also

been used as a photocatalyst to eliminate 100% of *E. coli* within 240 min in the presence of visible light. The performance of this graphitic carbon nitride nanosheet was better than that of bulk graphitic carbon nitride because the bulk graphitic carbon nitride could only eliminate 77.1% of the bacteria under the same conditions [23]. In a similar research, 5 log and 3 log of the *E. coli* were killed when nanosheet and bulk graphitic carbon nitride were respectively used as a photocatalyst in the presence of visible light radiation. When a single layer of the graphitic carbon nitride was used, 2×10^7 cfu mL⁻¹ was inactivated under the same conditions [19]. Another metal-free photocatalyst that has been used as an effective photocatalyst against *E. coli* is graphene quantum dot. Electrochemical techniques have been used to produce graphene quantum dots which killed *E. coli* by damaging the cell membrane in the presence of light. The killing of the bacteria was confirmed by the use of the plate count method, where the amount of propidium iodide that was consumed was used for the estimation. When the experiment was repeated under the same conditions in the absence of light, no inactivation took place. In addition, the use of ordinary light for the inactivation was not effective against the bacteria strains [83].

3.6. Inactivation of *E. coli* by Metal Doped Photocatalysts

Divalent cobalt was used to dope microsphere nanostructure of BiOBr_xCl_{1-x} and the photocatalyst showed good photocatalytic *E. coli* inactivation. The good photocatalytic performance was attributed to the enhanced charge separation and good light absorptivity as a result of cobalt doping [84]. The doping of divalent cobalt into bismuth was effective as a result of the abundance of cobalt and the fact that the size of divalent cobalt (0.65 Å) is comparatively smaller than the size of trivalent bismuth (1.03 Å), which made the incorporation of divalent cobalt into the lattice structure of BiOBr easy [84,85]. In another investigation, iron was used to dope polyaniline to form a metal organic framework which was used as photocatalyst for the inactivation of *E. coli*. Evidence from electron paramagnetic resonance, fluorescent test and quenching experiments revealed that h⁺, ·OH, ·O₂⁻ and e⁻ are the reacting species that aided the photocatalytic inactivation of bacteria with hydroxyl radicals being the most predominant [86]. Gold has also been used to dope nanoparticles of titanium oxide through the seed growth method. The catalytic activity of titanium oxide improved significantly as a result of the presence of gold as the doping agent, and it reflected in the inactivation of bacteria better than when pure titanium oxide was used as photocatalyst under UV light [87]. Silver, another noble metal, was used to dope oxides of iron to form a composite photocatalyst that was used to inactivate *E. coli* in the presence of light [88]. Iron has been used to dope ZnO nanoparticles, and the bandgap of Fe-doped zinc oxide was found to be lower than the band gap energy of undoped zinc oxide. This doped photocatalyst was active against *E. coli* in the presence of sunlight.

3.7. Inactivation of *E. coli* by Photocatalysts Doped with Non-Metal

Sulphur, nitrogen, phosphorus and carbon have been used to dope series of photocatalysts in order to improve their photocatalytic efficiency [89,90]. For instance, titanium oxide doped with nitrogen was used as an active photocatalyst against *E. coli*. The performance of this photocatalyst increased when carbon, another non-metal, was used to sensitize the photocatalyst. After 60 min of visible light irradiation, approximately 80% *E. coli* was eliminated, and this could be attributed to the lowering of band gap as a result of the introduction of non-metals [91]. Raisada et al. [92] doped silver vanadate and graphitic carbon nitride composite with sulphur and phosphorus. The presence of these non-metal dopants achieved 99% of *E. coli* inactivation within 1 h in the presence of visible light radiation.

3.8. Inactivation of *E. coli* by Heterojunction Systems

One of the most common heterojunction systems is the type II heterojunction system, which is formed by two semiconductors (SC I and SC II) that possess wide and narrow band gaps, respectively. The valence band and the conduction band of semiconductor 1 (SC I)

are more than the valence band and the conduction band of semiconductor 2 (SC II). This makes it possible for photo-induced holes to move from the valence band of SC I to the valence band of SC II, whereas the light-excited electrons will migrate in the reverse direction (SC I to SC II). The movement in different direction boosts the charge separation, which culminate in better photocatalytic performance. Another common heterojunction system is the Z-scheme heterojunction system [93]. The Z-scheme and other heterojunction schemes are illustrated in Figure 4a–f and it could be with or without semiconductor at its interface. The semiconductor acts as the electron mediator for charge relay and recombination. Without the mediator, the photo-excited charge in the valence band of SC I recombine with the low-lying conduction band of SC II at the interface of SC I and SC II [94]. The s-scheme has also been reported as another heterojunction system. In the s-scheme heterojunction system, two n-type semiconductors with different band structures are combined together. One of the photocatalyst is the oxidation photocatalyst, while the other one is the reduction photocatalyst [95]. The Schottky scheme has equally been reported as another way of improving the photocatalytic efficiency of the photocatalysts. In this heterojunction, a semiconductor makes contact with a metal to generate a potential difference known as the Schottky barrier. The generation of this potential difference is as a result of non-similar Fermi levels and work function between the semiconductor and the metal. The Schottky barrier function elongates the lifespan of the electron by preventing the recombination of the charge carriers [96,97].

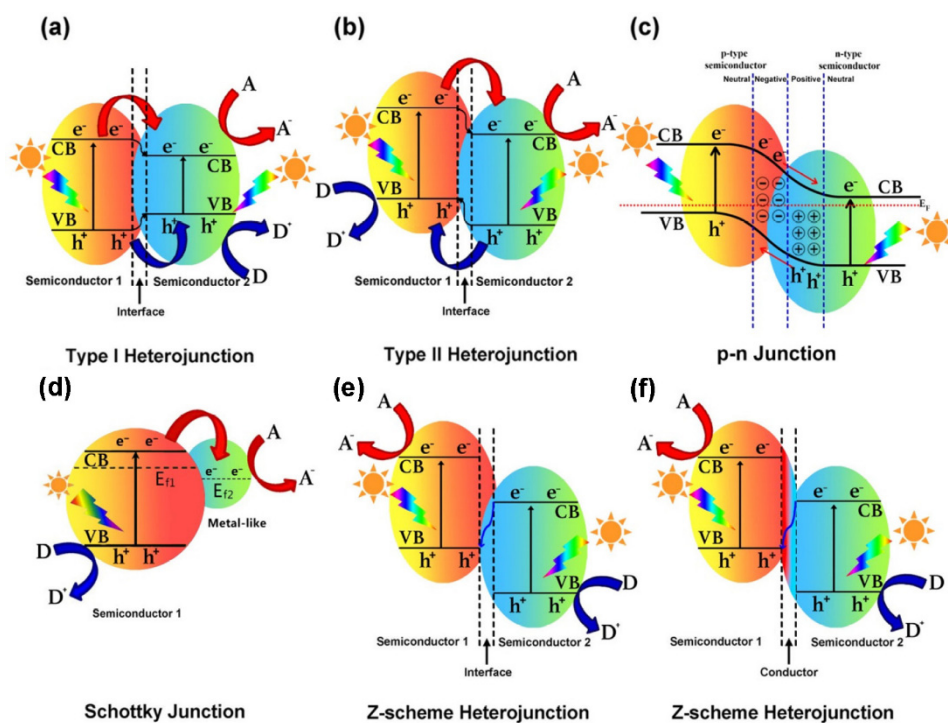


Figure 4. Examples of heterojunction systems. Reproduced from [98], Copyright (2019), with permission from Elsevier.

The combination of nano- Ag_2ZrO_3 and graphitic carbon nitride has been used to fabricate a type II heterojunction system and the resultant photocatalyst was used for eliminating gram-negative *E. coli*. Exposure of the *E. coli* to visible light in the presence of this heterojunction photocatalysts led to the reduction of the population of *E. coli* to 3%, but longer exposure time achieved a reduction of the *E. coli* to 1.27% [99]. The Z-scheme heterojunction system made from silver iodide and organic framework having a covalent bond was also investigated for photocatalytic inactivation of *E. coli*. The inactivation was affected under visible light irradiation by the hydroxyl radicals, holes and peroxy radical as revealed by the scavenger experiment [100]. Complete bacteria disinfection

(1.5×10^6 CFU mL⁻¹) was achieved in 40 min when visible light was used, unlike in the dark where there was no inactivation of viable cells. After four cycles of using the photocatalyst, there was still complete inactivation of the bacteria, which shows that the photocatalyst was reusable [100]. Another Z-scheme heterojunction system that was used for the inactivation of *E. coli* under visible light irradiation was made from nanocomposites of AgI/Bi₂Sn₂O₇. The investigation by electron spin resonance and radical trapping experiments showed that 7.48-log of the bacteria was inactivated via ·OH, ·O₂⁻, e⁻ and h⁺ [101]. The Z-scheme heterojunction made from graphitic carbon nitride and nickel phosphide was also used to inactivate *E. coli* via the oxidation by holes in the presence of visible light. The number of *E. coli* inactivated with this Z-scheme heterojunction system was 10-fold better than the number inactivated with neat graphitic carbon nitride and graphitic carbon nitride doped with platinum [102]. Ju et al. [103] fabricated a Z-scheme ternary heterojunction system made from Ag doped AgVO₃ and BiVO₄ assisted by polyvinylpyrrolidone. This photocatalyst displayed a good photocatalytic performance for the inactivation of *E. coli* through the action of peroxide radicals and holes generated under visible light irradiation. The Z-scheme heterojunction system of graphene aerogel, bismuth vanadate, silver chloride and silver which was made by a hydrothermal technique. The formation of Z-scheme heterojunction boosted both the charge transfer and separation of electrons. This photocatalyst displayed total inactivation of all the *E. coli* in the system in less than 25 min in the presence of visible light irradiation [104].

Finally, one other strategy was adopted to reduce the recombination of holes and electrons and obtain a better activity during photocatalysis is the formation of the p-n heterojunction system [105]. *E. coli* has also been inactivated by the p-n heterojunction photocatalysts, made from polyaniline and zinc oxide. The improved photocatalytic performance of this photocatalyst was linked to the synergistic effect of the p-n heterojunction as well as the generation of hydroxyl and peroxy radicals assisted by relatively large surface area of the photocatalysts [106]. Examples of other recent studies on the photocatalytic inactivation of *E. coli* are shown in Table 1.

Table 1. Recent studies on the photocatalytic inactivation of *E. coli*.

Photocatalyst	Fabrication Method	Performance	Light Used	Reactive Species	Ref.
MXene/ anatase TiO ₂ loaded in reactor made from polyurethane foam	-	3.4 lg order better than 2.5 lg order obtained with UV alone	Ultraviolet	e ⁻ , HO· and h ⁺	[107]
Cu ₂ O on cotton fibers	In-situ synthesis	93.25% <i>E. coli</i> inactivation	350 W xenon lamp	·OH, O ₂ ·e ⁻ , h ⁺	[108]
Metallic silver on Pinewood biochar support	One-step carbothermal reduction	Good <i>E. coli</i> inactivation efficiency	Ultraviolet	¹ O ₂ , ·OH, ·O ₂ ⁻ , e ⁻ , h ⁺	[109]
Composites made from zeolite and titania Fe ₃ O ₄ @SiO ₂ @ZnO-Ag ₃ PO ₄	Solid-state dispersion	40% <i>E. coli</i> reduction in 1 h	Ultraviolet	O ₂ ⁻	[110]
	Hydrothermal		Visible light	·OH, O ₂ ·e ⁻ , h ⁺	[111]
Heterostructure of ZnO/CdS heterojunction	Hydrothermal	Better performance than ordinary ZnO	Visible light	OH·	[112]
Ag/TiO ₂ /ZnO composite	Hydrothermal	Better performance than ordinary ZnO	Visible light	O ₂ , ·OH	[113]
Heterostructure TiO ₂ /Ag ₃ PO ₄ /graphene oxide	Ion-exchange and electrostatically-driven assembly	Good performance	Solar light	·OH, h ⁺	[114]
Nanocomposites of Ag/Cu-cellulose	Chemical reduction	Active against <i>E. coli</i>	visible light	O ₂ ⁻ , h ⁺ and OH·	[115]
Reduced graphene oxide decorated with Ag/ZnO	Green synthesis	Good <i>E. coli</i> inactivation	Visible and UV using metal halide lamp	-	[116]

Table 1. Cont.

Photocatalyst	Fabrication Method	Performance	Light Used	Reactive Species	Ref.
conjugated polymer/ CuO nanoparticles	-	Better bacteria passivation when peroxymonosulphate was introduced to the polymer	UV-vis light	h^+ , O_2^- and H_2O_2	[117]
Nanotube of TiO ₂ /Cu _x O _y	Anodization method	Inactivation of 97% <i>E. coli</i> in 1 h	Visible light	e^- , h^+ , $\cdot OH$, and O_2^- radicals	[118]
TiO ₂ nanowire-sensitized quantum dots of Mn-CdS/ZnCuInSe/CuInS ₂	-	96% <i>E. coli</i> present in 50 cm ³ 10 ⁵ colony forming units ml ⁻¹ solution were killed in 50 min	visible light	$\cdot HO_2$, $\cdot OH$, H_2O_2 , $\cdot O_2^-$	[119]
AgBr/AgVO ₃	Hydrothermal process	99.997% bacterial inactivation	Visible light	$\cdot OH$	[71]

4. Inactivation of *E. coli* by Assisted Photocatalysis

Most studies referred to this method as photoelectrocatalysis. This combined technique is advantageous because it clearly separates the site of oxidation from the site of reduction, which reduces the crossover of the products [120]. In addition, the measurement of voltage and current from electrochemical method can serve as parameter for quantifying the rate of photocatalysis [120]. *Pseudomonas aeruginosa* and *Escherichia coli* were removed from rainwater by combining both photocatalysis and electrochemical methods. This was achieved by designing a photoelectrochemical reactor, which was placed under the sun. Evidence from culture-based analysis showed that 5.5-log of *E. coli* reduction was achieved [121]. The photoelectrocatalytic system made from nanotubes of titanium oxide that was doped with the combination of tin oxide, nanoparticles of silver and antimony was active against *E. coli*. Over 5-log bacteria elimination was reported when this system was used for inactivating *E. coli* within 60 min in the presence of light [122]. Mesones et al. [123] also reported the use of photoelectrochemical approach to inactivate *E. coli*, but this was achieved by using titanium oxide composites as the photocatalyst, while RuO_x/Ti was used as the anode. When only the electrochemical process was used, the active radical for the inactivation was hydroxyl radical. However, when it was combined with photocatalysis, the active species for the inactivation were chlorine species and hydroxyl radicals [124]. In addition to the use of electrochemical method for assisting photocatalysis, plasmon has also been used to aid photocatalysis for the inactivation of *E. coli* [125].

5. Quantitative Estimation of *Escherichia coli*

One of the most common methods for estimating *E. coli* is to use Ethidium monoazide bromide coupled with the quantitative polymerase chain reaction (EMA-qPCR) analysis. The method is used to validate other methods of *E. coli* estimation. The pre-treatment carried out on *E. coli* before carrying out the quantitative polymerase chain reaction involves the use of Ethidium monoazide bromide. This analysis works based on the membrane integrity of the bacteria. EMA binds to the DNA of the bacteria with damaged cell membrane and inhibits the bound DNA amplification when subjected to polymerase chain reaction. The amplification of the DNA would be done for bacteria cells with undamaged DNA [126]. The use of aerosol generator to estimate the population of *E. coli* has also been reported. The suspension of *E. coli* cells was aerosolized to less than 5 µm to give bioaerosol containing bacteria. This was followed by a plate counting step and incubation of nutrient agar at a temperature that is above room temperature for a day [107]. In some cases, the incubation is assisted with rotary shaker or centrifuge at a particular rotation per minute before termination of the incubation after some minutes [109]. The counting on each nutrient agar plate is expressed in colony-forming units (cfu) [107]. Transcriptome analysis is another method of estimating the amount of *E. coli*. This method requires the isolation of RNA of the bacteria before the concentration and purity of the bacteria cells

would be estimated by a spectrophotometer. The process is immediately followed by the use of bioanalyzer to determine the integrity of the RNA [56]. The use of fluorescence detector with 4'-6-diamidino-2-phenylindole has also been reported [122]. The working principle of this technique relies on the fact that 4'-6-diamidino-2-phenylindole stains the DNA of the bacteria with a damaged cell membrane. Since reactive oxygen species will damage the cell membrane of *E. coli* during photocatalysis, in order to achieve accurate results, the sample containing the bacteria was rinsed several times with saline-phosphate buffer. The mixture of the stain and the treated sample was then excited and quantified via the fluorescence detector [122]. Kayani et al. [111] described the disc diffusion method as an alternative method of quantifying *E. coli* inactivated by photocatalysis. The prepared sample was placed in a treated plate, and the plate was then exposed to visible light for less than 1 h and afterward inoculated for 10 h at 37 °C. An agar well diffusion method was also reported by Bauer et al. [127]. In this method, four small wells (diameter 0.8 mm) were dug and the stock solution of the photocatalyst was placed into the dug well, followed by the incubation above room temperature for one day while methanol was used as control [128]. The disc diffusion method is another method that was used to quantify bacteria cells, and it involves the growth of *E. coli* strains on Mueller–Hinton agar for 1 day at 37 °C, while shaking mildly. The zones without the growth of *E. coli* are described as the zone of inhibition, which is usually measured in millimeters [79]. Other methods are the micro-dilution method and colony-counting method [23,52]. Before the use of colony counting method, the bacteria cells are usually introduced into the solution of sodium chloride and spread onto nutrient agar, followed by incubation for a day [59]. *Limulus* tests have also been used in determining if the bacteria were inactivated. The test relies on the determination of the endotoxin cumulative content of *E. coli* in the samples [129].

6. Photocatalytic Systems Designed for *E. coli* Inactivation

Different photocatalytic set-ups have been used for the inactivation of *E. coli*, and one of them is the liquid-film system. In this set up, light is passed from the top of the set-up through a transparent pyrex window into the suspension of *E. coli*. The suspension is placed on the petri-dish holding a glass coated with the photocatalysts such as titanium oxide. The liquid-film set-up is different from the membrane separated system, where the light is passed from the base of the set-up through a normal glass support to the photocatalyst-coated glass, then to the membrane holding the suspension of *E. coli*. These two systems are shown in Figure 5a,b.

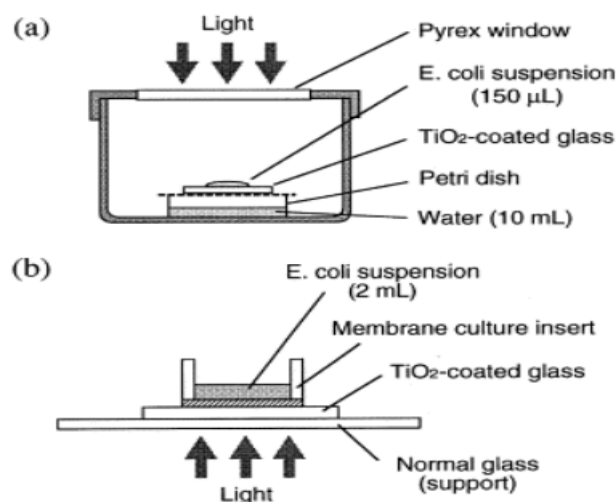


Figure 5. (a) Liquid-film photocatalytic system and (b) membrane-separated system. Reprinted from [59], Copyright (1997), with permission from Elsevier.

One other design allows the reduction and oxidation to take place simultaneously, and this makes the investigation of the photocatalytic inactivation to be possible. It is usually employed where a photocatalyst doped with metal is employed for *E. coli* inactivation. The metal dopant act as the reduction site, which boosts the photocatalytic efficiency via better light-generated charge separation [130]. In this design, the detector that is used is the carbon microelectrode, which is usually positioned close to the surface of the photocatalysts as shown in Figure 6a,b, where palladium doped with titanium oxide was used as the photocatalysts. Materials used to design the carbon microelectrode are copper wire, epoxy resin, mercury, carbon fiber and pyrex glass tube.

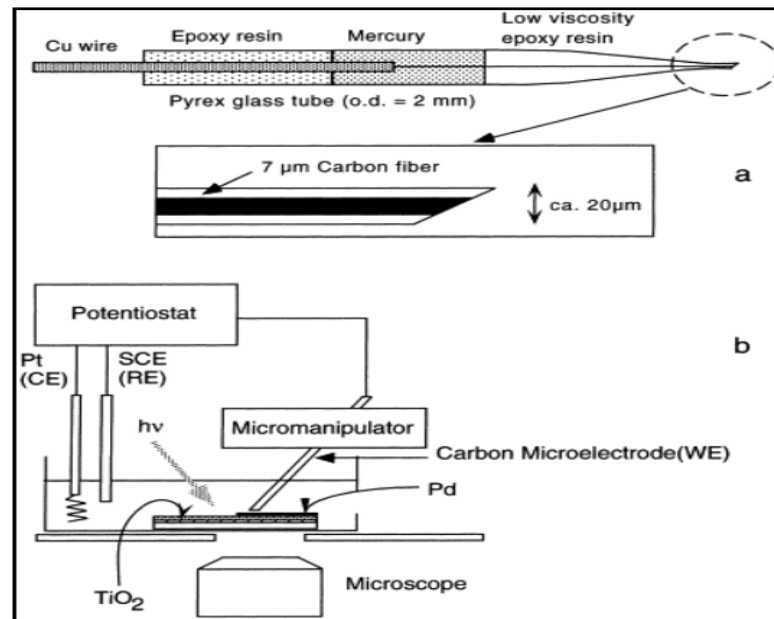


Figure 6. (a) The design of carbon microelectrode, (b) set-up for simultaneous monitoring of oxidation and reduction during *E. coli* inactivation. Reprinted from [130]. Copyright (2000), with permission from Elsevier.

Lu et al. [107] reported the use of photocatalyst-loaded reactor (Figure 7) made from polyurethane foam and quartz. The polyurethane was used as support that carried the photocatalyst in order to improve its contact area. The photo-reactor is cylindrical in shape, it has a double layer and is of considerable size (35 cm in length and 7 cm in diameter). This reactor has fitted sampler and flow meter to measure the movement of air and aerosol containing *E. coli* in the system.

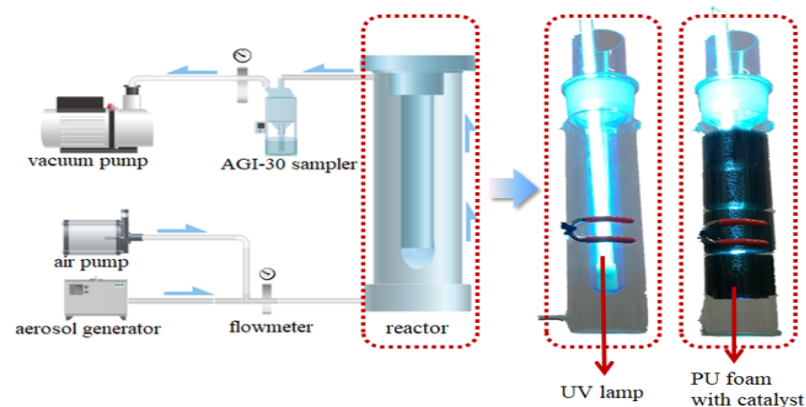


Figure 7. Polyurethane foam design for the inactivation of *E. coli*. Reprinted from [107], Copyright (2021), with permission from Elsevier.

A portable, easy-to-use photocatalytic design, based on the use of photoelectric has also been reported [131]. It was used to inactivate 5-log of *E. coli* within 10 s. This reactor has nanotube photoanode made from titanium oxide photocatalyst, which was formed into the shape of teacup, and it is powered by small-sized battery that is rechargeable. The battery is the source of energy for the light emitting diode fitted into the reactor. This novel photocatalytic design is shown in Figure 8.

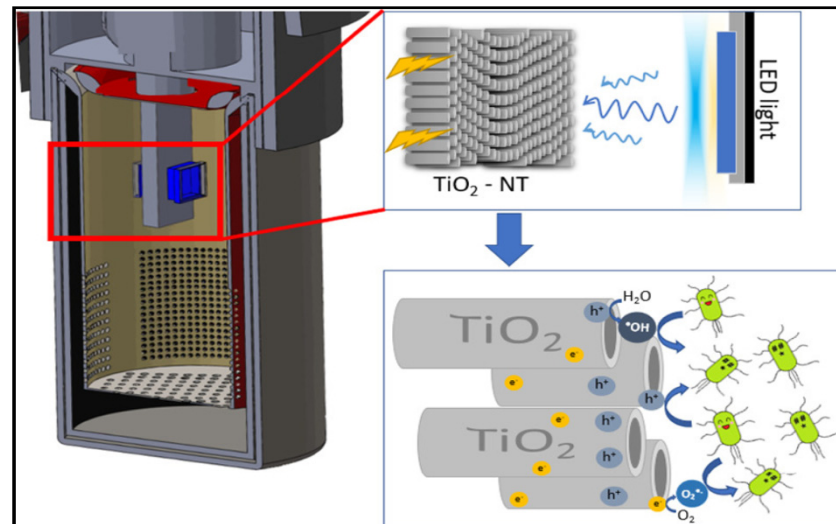


Figure 8. Photoelectric cup-like photocatalytic design for *E. coli* inactivation. Reprinted from [131], Copyright (2020), with permission from Elsevier.

A relatively new photoreactor set-up, which also utilizes light emitting diode as a source of illumination was designed with several fixed bed stages (Figure 9). The photocatalyst used for the design was titanium oxide nanoparticles doped with nitrogen, and the nanoparticles were rendered immobile on the beads made from glass. Each fixed bed was made from acrylic sheet with dimensions of 100 mm long, 50 mm wide and 15 mm high. The fixed bed stage was arranged such that there was gravitational flow from one stage to another stage and there was continuous flow of water in and out of the reactor. The suspension of *E. coli* is usually introduced into the first stage through a peristaltic pump. The incident photon flux in the set-up is usually measured by potassium ferrioxalate actinometer [132].

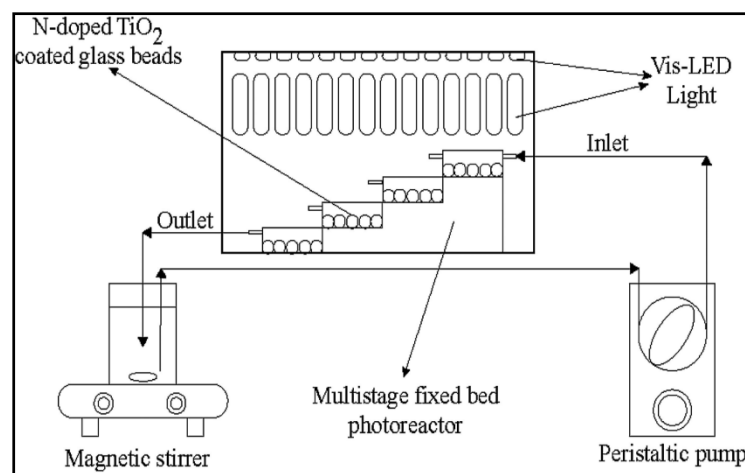


Figure 9. Multiple stage photoreactors for *E. coli* inactivation. Reprinted from [132], Copyright (2020), with permission from Elsevier.

Another design allows both *E. coli* and the photocatalysts to exist together in the buffer solution in an electrophotocatalytic system, and platinum wire is used as the electrode (Figure 10). The system was irradiated by an arc Xenon lamp, and the solution containing *E. coli* was continuously stirred for a particular period of time before a little sample of the solution was taken to determine the inactivation rate. This design requires the screening out of ultraviolet light (UVC and UVB) achieved by using a band filter. The intensity of light from the arc Xenon lamp was monitored by using a spectroradiometer [4].

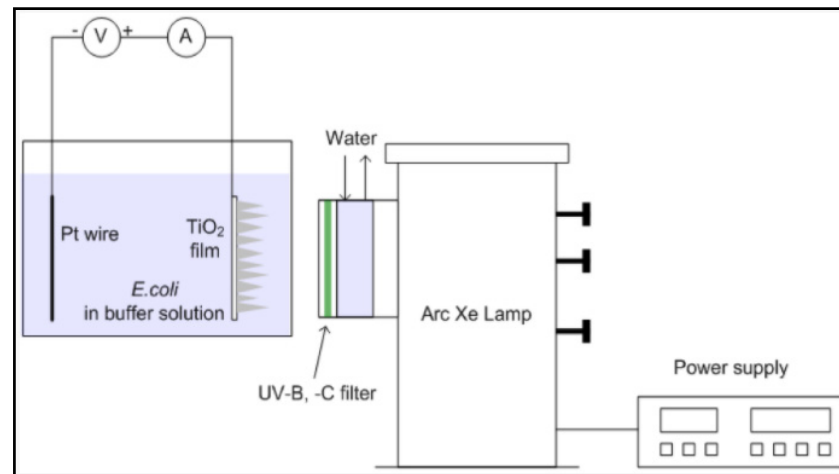


Figure 10. Photoelectrochemical and photocatalytic *E. coli* inactivation set-up [4]. Open access under creative common agreement (MDPI).

The quest to solve the problem of mass transfer in the photocatalytic reactors led to the design of simplified stirred-tank reactor [133]. This reactor was designed by putting a glass plate coated with the photocatalyst beneath a vessel having a water-jacketed wall that created a reservoir. Turbulent flow was generated within the reactor through the use of a stainless steel propeller that was rotated between 0–2500 rpm by a homogenator motor. The calibration of this homogenator motor was done by using an optical tachometer, and the mixing was enhanced by a baffle made from stainless steel [134]. This design is shown in Figure 11.

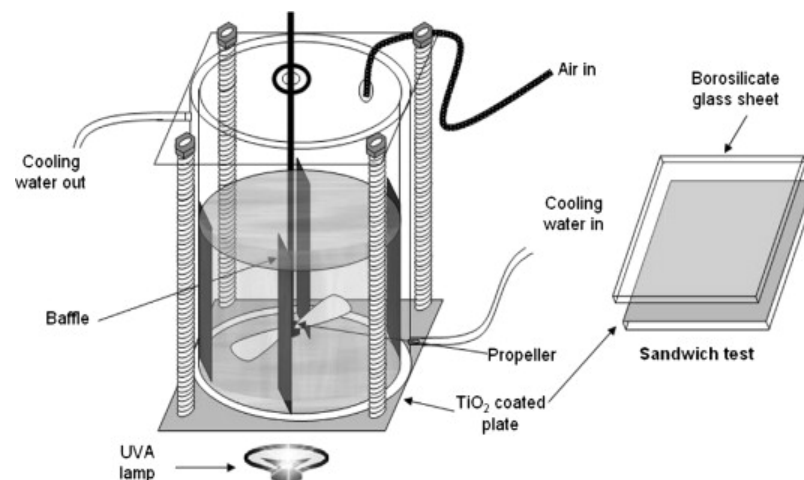


Figure 11. Stirred tank reactor for *E. coli* inactivation. Reprinted from [133], Copyright (2020), with permission from Elsevier.

7. Kinetics of the Inactivation of *E. coli* by Photocatalyst

The inactivation of *E. coli* depends on the intensity of light, the time of exposure to this light, and the initial population of the *E. coli* [135]. As expressed by Chick's law, there is a relationship between these factors; and the kinetics of *E. coli* inactivation usually follow first-order kinetics. The expression of Chick is presented in Equation (1):

$$N_t/N_0 = e^{(-kt)} \quad (1)$$

where l is the light intensity,

t is the exposure time,

N_0 is the initial population of *E. coli*,

N_t is the number of *E. coli* that survived after exposure to light,

K is the first-order rate constant.

Watson also worked along with Chick to form a Chick–Watson Model of inactivation (Equation (2)):

$$\log N_t/N_0 = -kt \quad (2)$$

where k is the inactivation rate at time, t .

Apart from the Chick and Watson models, the Hom model (Equation (3)) is another model used for the kinetics study of the inactivation of micro-organism, and this model was later modified to another model known as the modified-Hom model (Equation (4)) [132]:

$$\log N_t/N_0 = -kC^n T^m \quad (3)$$

$$\log N_t/N_0 = -K_1(1 - \exp - K_2 t)K_3 \quad (4)$$

where C is the load of the catalyst, m and n are empirical parameters, K is the inactivation rate and k_1, k_2, k_3 are constants of the modified-Hom Model.

Finally, the Weibull model is another simple model for investigating the kinetics of *E. coli* inactivation either in the presence or absence of heat. When UV light is used for the treatment, the sigmoidal curve for the inactivation will either be convex or concave, upward or downward when expressed as a function of UV dose or time of inactivation [136,137]:

$$\alpha\beta \log N_t/N_0 = -12.303t\alpha\beta \quad (5)$$

where α and β are the Weibull parameters, and these parameters are used to estimate the reliable time (t_R), which is an indication of the percentage of the bacteria that has been inactivated. The equation relating the reliable time with these parameters is presented in Equation (6) for a system that utilized UV light [137,138]:

$$\alpha\beta t_R = \alpha 2.3031\beta \quad (6)$$

8. Methods of Detecting *E. coli*

The detection of *E. coli* is necessary after the photocatalytic inactivation has been carried out in order to ascertain the treatment of the water from the *E. coli* contamination. One of the methods that has been used to detect the presence of *E. coli* is polymerase chain reactions (PCR). Other methods are biosensor-based techniques, immunology-based techniques, Fluorescence in Situ Hybridization (FISH), Pyrosequencing and Oligonucleotide Microarray. The principle of operations, merits and demerits of these methods are summarized in Table 2.

Table 2. Methods for detecting *E. coli*, their principle of operation, merits and demerits.

Detection Method	Principle of Operation	Merit	Demerit	Ref.
PCR	Specific target is amplified exponentially based on extension, annealing and denaturalization processes.	It is possible to detect multiple targets simultaneously in a single reaction; fast.	Accurate primer required to get correct results.	[139–141]
Multiplex PCR	Amplification of specific target	Its signal strength is not affected by the presence of <i>E. coli</i>	-	[100,142,143]
Quantitative real time PCR	Measurement of amplified product via rise in fluorescence	Post PCR-analysis not required; cross-contamination is reduced; fast, specific and sensitive	One pathogen only can be detected in a single reaction	[5,135,144]
Oligonucleotide Microarray	Detect mutation and gene expression at under changing condition via sophisticated genomic technology	Fast and simultaneous determination of all genes in a particular isolate is possible	Relatively expensive; lower specificity and sensitivity	[5,27,101]
Pyrosequencing	Monitoring of pyrophosphate liberated via bioluminescence and reaction of enzyme.	Numerous sequences can be read in one run	It requires concentrating the water pathogens before DNA extraction	[5,124,145,146]
Fluorescence in Situ Hybridization (FISH)	It involves the use of fluorescence dye and rRNA oligonucleotides hybridized with the sample.	Identification and detection can be achieved in a short time.	Treatment and concentration are required; low sensitivity; results may be altered by inhibitor increase during pre-treatment.	[5,139,140,147]
Immunology-Based Methods	It is based on the interaction of antigen and antibody which involve the use of monoclonal and polyclonal antibodies.	Multiple pathogens can be detected at once.	Cross-reactivity of antigens; low sensitivity, pre-treatment required.	[5,140,148,149]
Biosensor Based Methods	Recognition of the target analyte by using a bioreceptor and transducer	Possibility of automation; short time for analysis; portable and sample pre-treatment not required	Its sensitivity is affected by change in pH, temperature and mass.	[5,140,150–152]

PCR is polymerase chain reaction.

9. Conclusions and Recommendations

Contamination of water by pathogens poses a serious challenge to the health and well-being of both humans and animals. Hence, their presence in water must be examined often and the total elimination should be ensured in order to minimize different water-borne diseases. The total elimination of *E. coli* from drinking water could be achieved through the photocatalytic inactivation. New methods of testing and quantifying the *E. coli* load in water continues to emerge and studies continue to explore different ways of designing simple and cheap photocatalytic reactor. A detection method that could combine all the merits of the present *E. coli* detectors (fast, sensitive, does not require pretreatment, portable and can handle multiple targets in a single run) need to be investigated. In addition, a lot of effort needs to be channeled towards optimizing photocatalytic processes so that it will be more effective and practicable in the large scale because most of the reported works are still at the laboratory scale. Furthermore, extended investigations are needed in order to explore avenues for the immobilization of photocatalysts in order to prevent leaching into the water. The leaching of the nanoparticles into water could be prevented by introducing catalyst support. This will also prevent the aggregation and dispersal of the photocatalyst into the water, which may lead to secondary pollution. Finally, the use of

type II and Z-scheme heterojunction system for the inactivation of *E. coli* has been reported by several studies, but little attention was paid to the use of S-scheme, p-n heterojunction and Schottky heterojunction systems.

Author Contributions: All the authors contributed equally to the writing of this review article and therefore consent to the publication. All authors have read and agreed to the published version of the manuscript.

Funding: This research was funded by the National Research Foundation (NRF), South Africa, Grant Numbers (UID109333 and UID 116,338). The APC was funded by North-West University, South Africa.

Institutional Review Board Statement: Not applicable.

Informed Consent Statement: Not applicable.

Data Availability Statement: Not applicable.

Acknowledgments: The authors gratefully acknowledge the North-West University and the National Research Foundation, South Africa for providing financial assistance.

Conflicts of Interest: The authors declare no conflict of interest.

References

1. Odonkor, S.T.; Ampofo, J.K. *Escherichia coli* as an indicator of bacteriological quality of water: An overview. *Microbiol. Res.* **2013**, *4*, 2. [CrossRef]
2. Mahvi, A.H.; Farokhneshat, F.; Jamali, Y. Carcinogenic and Non-Carcinogenic Risk Assessment of Chromium in Drinking Water Sources: Birjand, Iran. *Res. J. Environ. Toxicol.* **2016**, *10*, 166–171. [CrossRef]
3. De Vietro, N.; Tursi, A.; Beneduci, A.; Chidichimo, F.; Milella, A.; Fracassi, F.; Chatzisyneon, E.; Chidichimo, G. Photocatalytic inactivation of *Escherichia coli* bacteria in water using low pressure plasma deposited TiO₂ cellulose fabric. *Photochem. Photobiol. Sci.* **2019**, *18*, 2248–2258. [CrossRef] [PubMed]
4. Park, J.; Kettleison, E.; An, W.-J.; Tang, Y.J.; Biswas, P. Inactivation of *E. Coli* in Water Using Photocatalytic, Nanostructured Films Synthesized by Aerosol Routes. *Catalysts* **2013**, *3*, 247–260. [CrossRef]
5. Ramírez-Castillo, F.Y.; Loera-Muro, A.; Jacques, M.; Garneau, P.; Avelar-González, F.J.; Harel, J.; Guerrero-Barrera, A.L. Waterborne Pathogens: Detection Methods and Challenges. *Pathogens* **2015**, *4*, 307–334. [CrossRef]
6. Carrillo-Gómez, J.; Durán-Acevedo, C.; García-Rico, R. Concentration Detection of the *E. coli* Bacteria in Drinking Water Treatment Plants through an E-Nose and a Volatiles Extraction System (VES). *Water* **2019**, *11*, 774. [CrossRef]
7. WHO. *Drinking-Water*; World Health Organization: Geneva, Switzerland, 2020.
8. Khani, M.; Amin, N.A.S.; Hosseini, S.N.; Heidarrezaei, M. Kinetics study of the photocatalytic inactivation of *Escherichia coli*. *Int. J. Nano Biomater.* **2016**, *6*, 139–150. [CrossRef]
9. Li, G.; Nie, X.; Chen, J.; Jiang, Q.; An, T.; Wong, P.K.; Zhang, H.; Zhao, H.; Yamashita, H. Enhanced visible-light-driven photocatalytic inactivation of *Escherichia coli* using g-C₃N₄/TiO₂ hybrid photocatalyst synthesized using a hydrothermal-calcination approach. *Water Res.* **2015**, *86*, 17–24. [CrossRef]
10. Edberg, S.; Rice, E.; Karlin, R.; Allen, M. *Escherichia coli*: The best biological drinking water indicator for public health protection. *J. Appl. Microbiol.* **2000**, *88*, 106S–116S. [CrossRef]
11. Bagundol, T.B.; Awa, A.L.; Enguito, M.R.C. Efficiency of Slow Sand Filter in Purifying Well Water. *J. Multidiscip. Stud.* **2013**, *2*. [CrossRef]
12. Rizzo, L.V.; Sannino, D.; Vaiano, V.; Sacco, O.; Scarpa, A.; Pietrogiamomi, D. Effect of solar simulated N-doped TiO₂ photocatalysis on the inactivation and antibiotic resistance of an *E. coli* strain in biologically treated urban wastewater. *Appl. Catal. B Environ.* **2014**, *144*, 369–378. [CrossRef]
13. Ribeiro, M.A.; Cruz, J.M.; Montagnolli, R.N.; Bidoia, E.D.; Lopes, P.R.M. Photocatalytic and photoelectrochemical inactivation of *Escherichia coli* and *Staphylococcus aureus*. *Water Supply* **2014**, *15*, 107–113. [CrossRef]
14. Szewzyk, U.; Manz, W.; Schleifer, K.-H. Microbiological Safety of Drinking Water. *Annu. Rev. Microbiol.* **2000**, *54*, 81–127. [CrossRef] [PubMed]
15. Benabbou, A.K.; Derriche, Z.; Felix, C.; Lejeune, P.; Guillard, C. Photocatalytic inactivation of *Escherichia coli*: Effect of concentration of TiO₂ and microorganism, nature, and intensity of UV irradiation. *Appl. Catal. B Environ.* **2007**, *76*, 257–263. [CrossRef]
16. Rojviroon, T.; Sirivithayapakorn, S. *E. coli* Bacteriostatic Action Using TiO₂ Photocatalytic Reactions. *Int. J. Photoenergy* **2018**, *2018*, 8474017. [CrossRef]
17. Dunlop, P.S.M.; Ciavola, M.; Rizzo, L.V.; McDowell, D.; Byrne, J. Effect of photocatalysis on the transfer of antibiotic resistance genes in urban wastewater. *Catal. Today* **2015**, *240*, 55–60. [CrossRef]
18. Friedman, N.; Temkin, E.; Carmeli, Y. The negative impact of antibiotic resistance. *Clin. Microbiol. Infect.* **2016**, *22*, 416–422. [CrossRef]

19. Zhao, H.; Yu, H.; Quan, X.; Chen, S.; Zhang, Y.; Zhao, H.; Wang, H. Fabrication of atomic single layer graphitic-C3N4 and its high performance of photocatalytic disinfection under visible light irradiation. *Appl. Catal. B Environ.* **2014**, *152–153*, 46–50. [[CrossRef](#)]
20. Muellner, M.G.; Wagner, E.D.; McCalla, K.; Richardson, S.D.; Woo, Y.-T.; Plewa, M.J. Haloacetonitriles vs. Regulated Haloacetic Acids: Are Nitrogen-Containing DBPs More Toxic? *Environ. Sci. Technol.* **2007**, *41*, 645–651. [[CrossRef](#)]
21. Tobaldi, D.M.; Piccirillo, C.; Rozman, N.; Pullar, R.; Seabra, M.; Škapin, A.S.; Castro, P.; Labrincha, J. Effects of Cu, Zn and Cu-Zn addition on the microstructure and antibacterial and photocatalytic functional properties of Cu-Zn modified TiO₂ nano-heterostructures. *J. Photochem. Photobiol. A: Chem.* **2016**, *330*, 44–54. [[CrossRef](#)]
22. Ahmad, R.; Ahmad, Z.; Khan, A.U.; Mastoi, N.R.; Kumar, G.; Kim, J. Photocatalytic systems as an advanced environmental remediation: Recent developments, limitations and new avenues for applications. *J. Environ. Chem. Eng.* **2016**, *4*, 4143–4164. [[CrossRef](#)]
23. Xu, J.; Wang, Z.; Zhu, Y. Enhanced Visible-Light-Driven Photocatalytic Disinfection Performance and Organic Pollutant Degradation Activity of Porous g-C3N4 Nanosheets. *ACS Appl. Mater. Interfaces* **2017**, *9*, 27727–27735. [[CrossRef](#)]
24. Delaram, D. *Escherichia Coli*. 2013. Available online: <http://ymbiodelaramdescherichiacoli.weebly.com/structure--function.html> (accessed on 17 November 2020).
25. Elena, S.F.; Whittam, T.S.; Winkworth, C.L.; Riley, M.A.; Lenski, R.E. Genomic divergence of *Escherichia coli* strains: Evidence for horizontal transfer and variation in mutation rates. *Int. Microbiol.* **2005**, *8*, 271–278.
26. Adamu, M.; Shamsul, B.; Desa, M.; Khairani-Bejo, S. A review on *Escherichia coli* O157: H7-the super pathogen. *Health* **2014**, *5*, 118–134.
27. Bruant, G.; Maynard, C.; Bekal, S.; Gaucher, I.; Masson, L.; Brousseau, R.; Harel, J. Development and Validation of an Oligonucleotide Microarray for Detection of Multiple Virulence and Antimicrobial Resistance Genes in *Escherichia coli*. *Appl. Environ. Microbiol.* **2006**, *72*, 3780–3784. [[CrossRef](#)]
28. Lupindu, A.M. *Isolation and Characterization of Escherichia Coli from Animals, Humans, and Environment*; Samie, A., Ed.; IntechOpen Limited: London, UK, 2017; pp. 187–206.
29. Kuhnert, P.; Nicolet, J.; Frey, J. Rapid and accurate identification of *Escherichia coli* K-12 strains. *Appl. Environ. Microbiol.* **1995**, *61*, 4135–4139. [[CrossRef](#)]
30. Beneduce, L.; Spano, G.; Massa, S. *Escherichia coli* O157: H7 general characteristics, isolation and identification techniques. *Ann. Microb.* **2003**, *53*, 511–528.
31. Luo, C.; Hu, G.; Zhu, H. Genome reannotation of *Escherichia coli* CFT073 with new insights into virulence. *BMC Genom.* **2009**, *10*, 552. [[CrossRef](#)]
32. Welch, R.A.; Burland, V.; Plunkett, G.; Redford, P.; Roesch, P.; Rasko, D.; Buckles, E.L.; Liou, S.-R.; Boutin, A.; Hackett, J.; et al. Extensive mosaic structure revealed by the complete genome sequence of uropathogenic *Escherichia coli*. *Proc. Natl. Acad. Sci. USA* **2002**, *99*, 17020–17024. [[CrossRef](#)]
33. Ajiboye, T.O.; Kuvarega, A.T.; Onwudiwe, D.C. Recent Strategies for Environmental Remediation of Organochlorine Pesticides. *Appl. Sci.* **2020**, *10*, 6286. [[CrossRef](#)]
34. Ajiboye, T.O.; Oyewo, O.A.; Onwudiwe, D.C. Simultaneous removal of organics and heavy metals from industrial wastewater: A review. *Chemosphere* **2021**, *262*, 128379. [[CrossRef](#)]
35. Wu, P.; Imlay, J.A.; Shang, J.K. Mechanism of *Escherichia coli* inactivation on palladium-modified nitrogen-doped titanium dioxide. *Biomater.* **2010**, *31*, 7526–7533. [[CrossRef](#)]
36. Cho, M.; Chung, H.; Choi, W.; Yoon, J. Linear correlation between inactivation of *E. coli* and OH radical concentration in TiO₂ photocatalytic disinfection. *Water Res.* **2004**, *38*, 1069–1077. [[CrossRef](#)]
37. Bekbolet, M.; Araz, C.V. Inactivation of *Escherichia coli* by photocatalytic oxidation. *Chemosphere* **1996**, *32*, 959–965. [[CrossRef](#)]
38. Pang, X.; Skillen, N.; Gunaratne, N.; Rooney, D.W.; Robertson, P.K. Removal of phthalates from aqueous solution by semiconductor photocatalysis: A review. *J. Hazard. Mater.* **2021**, *402*, 123461. [[CrossRef](#)]
39. Matsunaga, T.; Tomoda, R.; Nakajima, T.; Wake, H. Photoelectrochemical sterilization of microbial cells by semiconductor powders. *FEMS Microbiol. Lett.* **1985**, *29*, 211–214. [[CrossRef](#)]
40. Saito, T.; Iwase, T.; Horie, J.; Morioka, T. Mode of photocatalytic bactericidal action of powdered semiconductor TiO₂ on mutants streptococci. *J. Photochem. Photobiol. B Biol.* **1992**, *14*, 369–379. [[CrossRef](#)]
41. Zhang, C.; Li, Y.; Shuai, D.; Shen, Y.; Xiong, W.; Wang, L. Graphitic carbon nitride (g-C3N4)-based photocatalysts for water disinfection and microbial control: A review. *Chemosphere* **2019**, *214*, 462–479. [[CrossRef](#)]
42. Tsuji, I.; Kato, H.; Kobayashi, H.; Kudo, A. Photocatalytic H₂ Evolution Reaction from Aqueous Solutions over Band Structure-Controlled (AgIn)_xZn₂(1-x)S₂ Solid Solution Photocatalysts with Visible-Light Response and Their Surface Nanostructures. *J. Am. Chem. Soc.* **2004**, *126*, 13406–13413. [[CrossRef](#)]
43. Ong, W.-J.; Tan, L.-L.; Lling-Lling, T.; Yong, S.-T.; Chai, S.-P. Graphitic Carbon Nitride (g-C3N4)-Based Photocatalysts for Artificial Photosynthesis and Environmental Remediation: Are We a Step Closer To Achieving Sustainability? *Chem. Rev.* **2016**, *116*, 7159–7329. [[CrossRef](#)]
44. Zhao, Y.; Li, C.; Liu, X.; Gu, F.; Du, H.; Shi, L. Zn-doped TiO₂ nanoparticles with high photocatalytic activity synthesized by hydrogen-oxygen diffusion flame. *Appl. Catal. B Environ.* **2008**, *79*, 208–215. [[CrossRef](#)]

45. Reddy, B.M.; Reddy, G.K.; Rao, K.N.; Ganesh, I.; Ferreira, J.M. Characterization and photocatalytic activity of TiO₂-M_xO_y (M_xO_y = SiO₂, Al₂O₃, and ZrO₂) mixed oxides synthesized by microwave-induced solution combustion technique. *J. Mater. Sci.* **2009**, *44*, 4874–4882. [[CrossRef](#)]
46. Mishra, T.; Hait, J.; Aman, N.; Gunjan, M.; Mahato, B.; Jana, R. Surfactant mediated synthesis of spherical binary oxides photocatalytic with enhanced activity in visible light. *J. Coll. Interface Sci.* **2008**, *327*, 377–383. [[CrossRef](#)]
47. Zhang, X.; Lei, L. Preparation of photocatalytic Fe₂O₃-TiO₂ coatings in one step by metal organic chemical vapor deposition. *Appl. Surf. Sci.* **2008**, *254*, 2406–2412. [[CrossRef](#)]
48. Singh, J.; Khan, S.A.; Shah, J.; Kotnala, R.K.; Mohapatra, S. Nanostructured TiO₂ thin films prepared by RF magnetron sputtering for photocatalytic applications. *Appl. Surf. Sci.* **2017**, *422*, 953–961. [[CrossRef](#)]
49. Brayner, R.; Ferrari-Iliou, R.; Brivois, N.; Djediat, S.; Benedetti, M.F.; Fiévet, F. Toxicological Impact Studies Based on *Escherichia coli* Bacteria in Ultrafine ZnO Nanoparticles Colloidal Medium. *Nano Lett.* **2006**, *6*, 866–870. [[CrossRef](#)]
50. Ahmad, M.; Zaidi, S.J.A.; Zoha, S.; Khan, M.S.; Shahid, M.; Park, T.J.; Basit, M.A. Pseudo-SILAR assisted unique synthesis of ZnO/Ag₂O nanocomposites for improved photocatalytic and antibacterial performance without cytotoxic effect. *Coll. Surf. A Physicochem. Eng. Asp.* **2020**, *603*, 125200. [[CrossRef](#)]
51. Xie, Y.; Qu, X.; Li, J.; Li, D.; Wei, W.; Hui, D.; Zhang, Q.; Meng, F.; Yin, H.; Xu, X.; et al. Ultrafast physical bacterial inactivation and photocatalytic self-cleaning of ZnO nanoarrays for rapid and sustainable bactericidal applications. *Sci. Total. Environ.* **2020**, *738*, 139714. [[CrossRef](#)]
52. Rafique, M.; Tahir, M.B.; Irshad, M.; Nabi, G.; Gillani, S.S.A.; Iqbal, T.; Mubeen, M. Novel Citrus aurantifolia Leaves Based Biosynthesis of Copper Oxide Nanoparticles for Environmental and Wastewater Purification as an Efficient Photocatalyst and Antibacterial Agent. *Optik* **2020**, *219*, 165138. [[CrossRef](#)]
53. Amina, M.; Al Musayeib, N.M.; Alarfaj, N.A.; El-Tohamy, M.F.; Oraby, H.F.; Al Hamoud, G.A.; Bukhari, S.I.; Moubayed, N.M.S. Biogenic green synthesis of MgO nanoparticles using *Saussurea costus* biomasses for a comprehensive detection of their antimicrobial, cytotoxicity against MCF-7 breast cancer cells and photocatalysis potentials. *PLoS ONE* **2020**, *15*, e0237567. [[CrossRef](#)]
54. Adil, S.F.; Assal, M.E.; Khan, M.; Al-Warthan, A.; Siddiqui, M.R.H.; Liz-Marzán, L.M. Biogenic synthesis of metallic nanoparticles and prospects toward green chemistry. *Dalton Trans.* **2015**, *44*, 9709–9717. [[CrossRef](#)] [[PubMed](#)]
55. Li, Z.; Yang, T. The Application of Biomolecules in the Preparation of Nanomaterials. *Biomed. Eng. Front. Chall.* **2011**, *319*. [[CrossRef](#)]
56. Guan, G.; Zhang, L.; Zhu, J.; Wu, H.; Li, W.; Sun, Q. Antibacterial properties and mechanism of biopolymer-based films functionalized by CuO/ZnO nanoparticles against *Escherichia coli* and *Staphylococcus aureus*. *J. Hazard. Mater.* **2021**, *402*, 123542. [[CrossRef](#)]
57. Hashimoto, K.; Irie, H.; Fujishima, A. TiO₂ Photocatalysis: A Historical Overview and Future Prospects. *Jpn. J. Appl. Phys.* **2005**, *44*, 8269–8285. [[CrossRef](#)]
58. Ahmed, F.; Awada, C.; Ansari, S.A.; Aljaafari, A.; Alshoaibi, A. Photocatalytic inactivation of *Escherichia coli* under UV light irradiation using large surface area anatase TiO₂ quantum dots. *R. Soc. Open Sci.* **2019**, *6*, 191444. [[CrossRef](#)] [[PubMed](#)]
59. Kikuchi, Y.; Sunada, K.; Iyoda, T.; Hashimoto, K.; Fujishima, A. Photocatalytic bactericidal effect of TiO₂ thin films: Dynamic view of the active oxygen species responsible for the effect. *J. Photochem. Photobiol. A Chem.* **1997**, *106*, 51–56. [[CrossRef](#)]
60. Wu, P.; Xie, R.; Imlay, K.; Shang, J.K. Visible-Light-Induced Bactericidal Activity of Titanium Dioxide Codoped with Nitrogen and Silver. *Environ. Sci. Technol.* **2010**, *44*, 6992–6997. [[CrossRef](#)]
61. Qiu, H.; Fang, S.; Huang, G.; Bi, J. A novel application of In₂S₃ for visible-light-driven photocatalytic inactivation of bacteria: Kinetics, stability, toxicity and mechanism. *Environ. Res.* **2020**, *190*, 110018. [[CrossRef](#)]
62. Hojamberdiev, M.; Piccirillo, C.; Cai, Y.; Kadirova, Z.C.; Yubuta, K.; Ruzimuradov, O. ZnS-containing industrial waste: Antibacterial activity and effects of thermal treatment temperature and atmosphere on photocatalytic activity. *J. Alloys Compd.* **2019**, *791*, 971–982. [[CrossRef](#)]
63. Wang, W.; Ng, T.W.; Ho, W.; Huang, J.; Liang, S.; An, T.; Li, G.; Yu, J.C.; Wong, P.K. CdIn₂S₄ microsphere as an efficient visible-light-driven photocatalyst for bacterial inactivation: Synthesis, characterizations and photocatalytic inactivation mechanisms. *Appl. Catal. B Environ.* **2013**, *129*, 482–490. [[CrossRef](#)]
64. Shan, J.; Li, X.; Yang, K.; Xiu, W.; Wen, Q.; Zhang, Y.; Yuwen, L.; Weng, L.; Teng, Z.; Song, C.Y. Efficient Bacteria Killing by Cu₂WS₄ Nanocrystals with Enzyme-like Properties and Bacteria-Binding Ability. *ACS Nano* **2019**, *13*, 13797–13808. [[CrossRef](#)] [[PubMed](#)]
65. Liu, F.; Nie, C.; Dong, Q.; Ma, Z.; Liu, W.; Tong, M. AgI modified covalent organic frameworks for effective bacterial disinfection and organic pollutant degradation under visible light irradiation. *J. Hazard. Mater.* **2020**, *398*, 122865. [[CrossRef](#)] [[PubMed](#)]
66. Li, M.; Liu, F.; Ma, Z.; Liu, W.; Liang, J.; Tong, M. Different mechanisms for *E. coli* disinfection and BPA degradation by CeO₂-AgI under visible light irradiation. *Chem. Eng. J.* **2019**, *371*, 750–758. [[CrossRef](#)]
67. Zhang, X.G.; Guan, D.L.; Niu, C.G.; Cao, Z.; Liang, C.; Tang, N.; Zhang, L.; Wen, X.J.; Zeng, G.M. Constructing magnetic and high-efficiency AgI/CuFe₂O₄ photocatalysts for inactivation of *Escherichia coli* and *Staphylococcus aureus* under visible light: Inactivation performance and mechanism analysis. *Sci. Total Environ.* **2019**, *668*, 730–742. [[CrossRef](#)]
68. Yang, Y.Y.; Niu, C.G.; Wen, X.J.; Zhang, L.; Liang, C.; Guo, H.; Guan, D.L.; Liu, H.Y.; Zeng, G.M. Fabrication of visible-light-driven silver iodide modified iodine-deficient bismuth oxyiodides Z-scheme heterojunctions with enhanced photocatalytic activity for *Escherichia coli* inactivation and tetracycline degradation. *J. Coll. Interface Sci.* **2019**, *533*, 636–648. [[CrossRef](#)]

69. Xu, Y.; Liu, Q.; Xie, M.; Huang, S.; He, M.; Huang, L.; Xu, H.; Li, H. Synthesis of zinc ferrite/silver iodide composite with enhanced photocatalytic antibacterial and pollutant degradation ability. *J. Coll. Interface Sci.* **2018**, *528*, 70–81. [[CrossRef](#)]
70. Guo, H.; Niu, C.G.; Zhang, L.; Wen, X.J.; Liang, C.; Zhang, X.G.; Guan, D.L.; Tang, N.; Zeng, G.M. Construction of Direct Z-Scheme AgI/Bi₂Sn₂O₇ Nanojunction System with Enhanced Photocatalytic Activity: Accelerated Interfacial Charge Transfer Induced Efficient Cr(VI) Reduction, Tetracycline Degradation and *Escherichia coli* Inactivation. *ACS Sustain. Chem. Eng.* **2018**, *6*, 8003–8018. [[CrossRef](#)]
71. Zhang, J.; Wang, J.; Xu, H.; Lv, X.; Zeng, Y.; Duan, J.; Hou, B. The effective photocatalysis and antibacterial properties of AgBr/AgVO₃ composites under visible-light. *RSC Adv.* **2019**, *9*, 37109–37118. [[CrossRef](#)]
72. Feng, T.; Liang, J.; Ma, Z.; Li, M.; Tong, M. Bactericidal activity and mechanisms of BiOBr-AgBr under both dark and visible light irradiation conditions. *Coll. Surfaces B Biointerfaces* **2018**, *167*, 275–283. [[CrossRef](#)]
73. Deng, J.; Liang, J.; Li, M.; Tong, M. Enhanced visible-light-driven photocatalytic bacteria disinfection by g-C₃N₄-AgBr. *Coll. Surfaces B Biointerfaces* **2017**, *152*, 49–57. [[CrossRef](#)]
74. Krutyakov, Y.A.; Zherebin, P.M.; Kudrinskiy, A.A.; Zubavichus, Y.V.; Presniakov, M.Y.; Yapryntsev, A.D.; Karabtseva, A.V.; Mikhaylov, D.M.; Lisichkin, G.V. New frontiers in water purification: Highly stable amphopolycarboxyglycinate-stabilized Ag-AgCl nanocomposite and its newly discovered potential. *J. Phys. D Appl. Phys.* **2016**, *49*, 375501. [[CrossRef](#)]
75. Brockway, L.; Vasiraju, V.; Asayesh-Ardakani, H.; Shahbazian-Yassar, R.; Vaddiraju, S. Thermoelectric properties of large-scale Zn₃P₂nanowire assemblies. *Nanotechnology* **2014**, *25*, 145401. [[CrossRef](#)] [[PubMed](#)]
76. Vance, C.C.; Vaddiraju, S.; Karthikeyan, R. Water disinfection using zinc phosphide nanowires under visible light conditions. *J. Environ. Chem. Eng.* **2018**, *6*, 568–573. [[CrossRef](#)]
77. Vasiraju, V.; Kang, Y.; Vaddiraju, S. Non-conformal decoration of semiconductor nanowire surfaces with boron nitride (BN) molecules for stability enhancement: Degradation-resistant Zn₃P₂, ZnO and Mg₂Si nanowires. *Phys. Chem. Chem. Phys.* **2014**, *16*, 16150. [[CrossRef](#)]
78. Karbasi, M.; Karimzadeh, F.; Raeissi, K.; Giannakis, S.; Pulgarin, C. Improving visible light photocatalytic inactivation of *E. coli* by inducing highly efficient radical pathways through peroxymonosulfate activation using 3-D, surface-enhanced, reduced graphene oxide (rGO) aerogels. *Chem. Eng. J.* **2020**, *396*, 125189. [[CrossRef](#)]
79. Tshangana, C.; Chabalala, M.; Muleja, A.A.; Nxumalo, E.; Mamba, B. Shape-dependant photocatalytic and antimicrobial activity of ZnO nanostructures when conjugated to graphene quantum dots. *J. Environ. Chem. Eng.* **2020**, *8*, 103930. [[CrossRef](#)]
80. Shanmugam, V.; Jeyaperumal, K.S.; Mariappan, P.; Muppudathi, A.L. Fabrication of novel g-C₃N₄based MoS₂and Bi₂O₃nanorod embedded ternary nanocomposites for superior photocatalytic performance and destruction of bacteria. *New J. Chem.* **2020**, *44*, 13182–13194. [[CrossRef](#)]
81. Liu, B.; Wu, Y.; Zhang, J.; Han, X.; Shi, H. Visible-light-driven g-C₃N₄/Cu₂O heterostructures with efficient photocatalytic activities for tetracycline degradation and microbial inactivation. *J. Photochem. Photobiol. A Chem.* **2019**, *378*, 1–8. [[CrossRef](#)]
82. Huang, J.; Ho, W.; Wang, X. Metal-free disinfection effects induced by graphitic carbon nitride polymers under visible light illumination. *Chem. Commun.* **2014**, *50*, 4338–4340. [[CrossRef](#)]
83. Ristic, B.Z.; Milenkovic, M.M.; Dakic, I.R.; Todorovic-Markovic, B.M.; Milosavljevic, M.S.; Budimir, M.D.; Paunovic, V.G.; Dramicanin, M.D.; Markovic, Z.M.; Trajkovic, V. Photodynamic antibacterial effect of graphene quantum dots. *Biomaterials* **2014**, *35*, 4428–4435. [[CrossRef](#)]
84. Cho, E.-C.; Chang-Jian, C.-W.; Huang, J.-H.; Lee, G.-Y.; Hung, W.-H.; Sung, M.-Y.; Lee, K.-C.; Weng, H.C.; Syu, W.-L.; Hsiao, Y.-S.; et al. Co²⁺-Doped BiOBr_xCl_{1-x} hierarchical microspheres display enhanced visible-light photocatalytic performance in the degradation of rhodamine B and antibiotics and the inactivation of *E. coli*. *J. Hazard. Mater.* **2021**, *402*, 123457. [[CrossRef](#)] [[PubMed](#)]
85. Huang, W.; Hua, X.; Zhao, Y.; Li, K.; Tang, L.; Zhou, M.; Cai, Z. Enhancement of visible-light-driven photocatalytic performance of BiOBr nanosheets by Co²⁺ doping. *J. Mater. Sci. Mater. Electron.* **2019**, *30*, 14967–14976. [[CrossRef](#)]
86. An, J.; Li, Y.; Chen, W.; Li, G.; He, J.; Feng, H. Electrochemically-deposited PANI on iron mesh-based metal-organic framework with enhanced visible-light response towards elimination of thiamphenicol and *E. coli*. *Environ. Res.* **2020**, *191*, 110067. [[CrossRef](#)] [[PubMed](#)]
87. Sagadevan, S.; Vennila, S.; Muthukrishnan, L.; Murugan, B.; Anita Lett, J.; Shahid, M.M.; Fatimah, I.; Akbarzadeh, O.; Mohammad, F.; Johan, M.R. Improved antimicrobial efficacy and photocatalytic performance of gold decorated titanium dioxide nanohybrid. *Optik* **2020**, *224*, 165515. [[CrossRef](#)]
88. Khan, A.U.; Rahman, A.U.; Yuan, Q.; Ahmad, A.; Khan, Z.U.H.; Mahnashi, M.H.; Alyami, B.A.; Alqahtani, Y.S.; Ullah, S.; Wirman, A.P. Facile and eco-benign fabrication of Ag/Fe₂O₃ nanocomposite using *Algaia Monozyga* leaves extract and its' efficient biocidal and photocatalytic applications. *Photodiagnosis Photodyn. Ther.* **2020**, *32*, 101970. [[CrossRef](#)]
89. Yu, J.C.; Ho, W.; Yu, J.; Yip, H.; Wong, P.K.; Zhao, J. Efficient Visible-Light-Induced Photocatalytic Disinfection on Sulfur-Doped Nanocrystalline Titania. *Environ. Sci. Technol.* **2005**, *39*, 1175–1179. [[CrossRef](#)]
90. Wu, P.; Shang, J.K. Visible-Light Inactivation of *Escherichia Coli* on N-Doped Titanium Oxide Thin Films. *MRS Online Proc. Libr.* **2006**, *930*, 210.
91. Li, Q.; Xie, R.; Li, Y.W.; Mintz, E.A.; Shang, J.K. Enhanced Visible-Light-Induced Photocatalytic Disinfection of *E. coli* by Carbon-Sensitized Nitrogen-Doped Titanium Oxide. *Environ. Sci. Technol.* **2007**, *41*, 5050–5056. [[CrossRef](#)]

92. Raizada, P.; Sudhaik, A.; Singh, P.; Shandilya, P.; Saini, A.K.; Gupta, V.K.; Lim, J.-H.; Jung, H.; Hosseini-Bandegharai, A. Fabrication of Ag₃VO₄ decorated phosphorus and sulphur co-doped graphitic carbon nitride as a high-dispersed photocatalyst for phenol mineralization and *E. coli* disinfection. *Sep. Purif. Technol.* **2019**, *212*, 887–900. [[CrossRef](#)]
93. Sasaki, Y.; Iwase, A.; Kato, H.; Kudo, A. The effect of co-catalyst for Z-scheme photocatalysis systems with an Fe³⁺/Fe²⁺ electron mediator on overall water splitting under visible light irradiation. *J. Catal.* **2008**, *259*, 133–137. [[CrossRef](#)]
94. Rhimi, B.; Wang, C.; Bahnemann, D.W. Latest progress in g-C₃N₄ based heterojunctions for hydrogen production via photocatalytic water splitting: A mini review. *J. Phys. Energy* **2020**, *2*, 042003. [[CrossRef](#)]
95. Fu, J.; Xu, Q.; Low, J.; Jiang, C.; Cheng, B. Ultrathin 2D/2D WO₃/g-C₃N₄ step-scheme H₂-production photocatalyst. *Appl. Catal. B Environ.* **2019**, *243*, 556–565. [[CrossRef](#)]
96. Li, G.; Gray, K.A. The solid–solid interface: Explaining the high and unique photocatalytic reactivity of TiO₂-based nanocomposite materials. *Chem. Phys.* **2007**, *339*, 173–187. [[CrossRef](#)]
97. Khan, M.R.; Chuan, T.W.; Yousuf, A.; Chowdhury, N.K.; Cheng, C.K. Schottky barrier and surface plasmonic resonance phenomena towards the photocatalytic reaction: Study of their mechanisms to enhance photocatalytic activity. *Catal. Sci. Technol.* **2015**, *5*, 2522–2531. [[CrossRef](#)]
98. Ren, Y.; Zeng, D.; Ong, W. Interfacial engineering of graphitic carbon nitride (g-C₃N₄)-based metal sulfide heterojunction photocatalysts for energy conversion: A review. *Chin. J. Catal.* **2019**, *40*, 289–319. [[CrossRef](#)]
99. Das, R.S.; Warkhade, S.K.; Kumar, A.; Gaikwad, G.; Wankhade, A.V. Graphitic carbon nitride @ silver zirconate nanocomposite (gC₃N₄@Ag₂ZrO₃): A Type-II heterojunction for an effective visible light photocatalysis and bacterial photo-inactivation. *J. Alloy. Compd.* **2020**, *846*, 155770. [[CrossRef](#)]
100. López-Saucedo, C.; Cerna, J.F.; Villegas-Sepulveda, N.; Thompson, R.; Velazquez, F.R.; Torres, J.; Tarr, P.I.; Estrada-García, T. Single multiplex polymerase chain reaction to detect diverse loci associated with diarrheagenic *Escherichia coli*. *Emerg. Infect. Dis.* **2003**, *9*, 127–131. [[CrossRef](#)]
101. Dallas, P.B.; Gottardo, N.G.; Firth, M.J.; Beesley, A.H.; Hoffmann, K.; Terry, P.A.; Freitas, J.R.; Boag, J.M.; Cummings, A.J.; Kees, U.R. Gene expression levels assessed by oligonucleotide microarray analysis and quantitative real-time RT-PCR – how well do they correlate? *BMC Genom.* **2005**, *6*, 59. [[CrossRef](#)]
102. Wang, W.; Ao, Z.; Li, G.; Xia, D.; Zhao, H.; Yu, J.C.; Wong, P.K. Earth-abundant Ni₂P/g-C₃N₄ lamellar nanohybrids for enhanced photocatalytic hydrogen evolution and bacterial inactivation under visible light irradiation. *Appl. Catal. B Environ.* **2017**, *217*, 570–580. [[CrossRef](#)]
103. Ju, P.; Wang, Y.; Sun, Y.; Zhang, D. In-situ green topotactic synthesis of a novel Z-scheme Ag@AgVO₃/BiVO₄ heterostructure with highly enhanced visible-light photocatalytic activity. *J. Coll. Interface Sci.* **2020**, *579*, 431–447. [[CrossRef](#)]
104. Lin, L.; Xie, Q.; Zhang, M.; Liu, C.; Zhang, Y.; Wang, G.; Zou, P.; Zeng, J.; Chen, H.; Zhao, M. Construction of Z-scheme Ag-AgBr/BiVO₄/graphene aerogel with enhanced photocatalytic degradation and antibacterial activities. *Coll. Surfaces A Physicochem. Eng. Asp.* **2020**, *601*, 124978. [[CrossRef](#)]
105. Jang, J.S.; Kim, H.G.; Lee, J.S. Heterojunction semiconductors: A strategy to develop efficient photocatalytic materials for visible light water splitting. *Catal. Today* **2012**, *185*, 270–277. [[CrossRef](#)]
106. Zou, T.; Wang, C.; Tan, R.; Song, W.; Cheng, Y. Preparation of pompon-like ZnO-PANI heterostructure and its applications for the treatment of typical water pollutants under visible light. *J. Hazard. Mater.* **2017**, *338*, 276–286. [[CrossRef](#)] [[PubMed](#)]
107. Lu, S.; Meng, G.; Wang, C.; Chen, H. Photocatalytic inactivation of airborne bacteria in a polyurethane foam reactor loaded with a hybrid of MXene and anatase TiO₂ exposing {001} facets. *Chem. Eng. J.* **2021**, *404*, 126526. [[CrossRef](#)]
108. Su, X.; Chen, W.; Han, Y.; Wang, D.; Yao, J. In-situ synthesis of Cu₂O on cotton fibers with antibacterial properties and reusable photocatalytic degradation of dyes. *Appl. Surf. Sci.* **2021**, *536*, 147945. [[CrossRef](#)] [[PubMed](#)]
109. Shi, J.; Wang, J.; Liang, L.; Xu, Z.; Chen, Y.; Chen, S.; Xu, M.; Wang, X.; Wang, S. Carbothermal synthesis of biochar-supported metallic silver for enhanced photocatalytic removal of methylene blue and antimicrobial efficacy. *J. Hazard. Mater.* **2021**, *401*, 123382. [[CrossRef](#)]
110. Wadhwa, S.; Mathur, A.; Pendurthi, R.; Singhal, U.; Khanuja, M.; Roy, S.S. Titania-based porous nanocomposites for potential environmental applications. *Bull. Mater. Sci.* **2020**, *43*, 47. [[CrossRef](#)]
111. Mao, K.; Zhu, Y.; Zhang, X.; Rong, J.; Qiu, F.; Chen, H.; Xu, J.; Yang, D.; Zhang, T. Effective loading of well-doped ZnO/Ag₃PO₄ nanohybrids on magnetic core via one step for promoting its photocatalytic antibacterial activity. *Coll. Surfaces A Physicochem. Eng. Asp.* **2020**, *603*, 125187. [[CrossRef](#)]
112. Xu, F.; Yuan, Y.; Han, H.; Wu, D.; Gao, Z.; Jiang, K. Synthesis of ZnO/CdS hierarchical heterostructure with enhanced photocatalytic efficiency under nature sunlight. *CrystrEngComm* **2012**, *14*, 3615–3622. [[CrossRef](#)]
113. Pant, H.R.; Pant, B.; Sharma, R.K.; Amarjargal, A.; Kim, H.J.; Park, C.H.; Tijing, L.D.; Kim, C.S. Antibacterial and photocatalytic properties of Ag/TiO₂/ZnO nano-flowers prepared by facile one-pot hydrothermal process. *Ceram. Int.* **2013**, *39*, 1503–1510. [[CrossRef](#)]
114. Yang, X.; Qin, J.; Jiang, Y.; Chen, K.; Yan, X.; Zhang, D.; Li, R.; Tang, H. Fabrication of P25/Ag₃PO₄/graphene oxide heterostructures for enhanced solar photocatalytic degradation of organic pollutants and bacteria. *Appl. Catal. B Environ.* **2015**, *166–167*, 231–240. [[CrossRef](#)]
115. Kokilavani, S.; Syed, A.; Thomas, A.M.; Elgorban, A.M.; Raju, L.L.; Das, A.; Khan, S.S. Facile synthesis of Ag/Cu-cellulose nanocomposite for detection, photocatalysis and anti-microbial applications. *Optik* **2020**, *220*, 165218. [[CrossRef](#)]

116. Belachew, N.; Kahsay, M.H.; Tadesse, A.; Basavaiah, K. Green synthesis of reduced graphene oxide grafted Ag/ZnO for photocatalytic abatement of methylene blue and antibacterial activities. *J. Environ. Chem. Eng.* **2020**, *8*, 104106. [[CrossRef](#)]
117. Djellabi, R.; Ali, J.; Zhao, X.; Saber, A.N.; Yang, B. CuO NPs incorporated into electron-rich TCTA@PVP photoactive polymer for the photocatalytic oxidation of dyes and bacteria inactivation. *J. Water Process. Eng.* **2020**, *36*, 101238. [[CrossRef](#)]
118. Kozak, M.; Mazierski, P.; Żebrowska, J.; Kobylański, M.; Klimczuk, T.; Lisowski, W.; Trykowski, G.; Nowaczyk, G.; Zaleska-Medynska, A. Electrochemically obtained TiO₂/Cux Oy nanotube arrays presenting a photocatalytic response in processes of pollutants degradation and bacteria inactivation in aqueous phase. *Catalysts* **2018**, *8*, 237. [[CrossRef](#)]
119. Kokilavani, S.; Syed, A.; Raju, L.L.; Al-Rashed, S.; Elgorban, A.M.; Thomas, A.M.; Das, A.; Khan, S.S. Citrate functionalized Ag NPs-polyethylene glycol nanocomposite for the sensitive and selective detection of mercury (II) ion, photocatalytic and antimicrobial applications. *Phys. E Low-Dimens. Syst. Nanostruct.* **2020**, *124*, 114335. [[CrossRef](#)]
120. Zhu, S.; Wang, D. Photocatalysis: Basic Principles, Diverse Forms of Implementations and Emerging Scientific Opportunities. *Adv. Energy Mater.* **2017**, *7*, 1700841. [[CrossRef](#)]
121. McMichael, S.; Waso, M.; Reyneke, B.; Khan, W.; Byrne, J.; Fernández-Ibáñez, P. Electrochemically Assisted Photocatalysis for the Disinfection of Rainwater under Solar Irradiation. *Appl. Catal. B Environ.* **2020**, *281*, 119485. [[CrossRef](#)]
122. He, H.; Sun, S.; Gao, J.; Huang, B.; Zhao, T.; Deng, H.; Wang, X.; Pan, X. Photoelectrocatalytic simultaneous removal of 17 α -ethinylestradiol and *E. coli* using the anode of Ag and SnO₂-Sb 3D-loaded TiO₂ nanotube arrays. *J. Hazard. Mater.* **2020**, *398*, 122805. [[CrossRef](#)]
123. Mesones, S.; Mena, E.; Muñoz, M.J.L.; Adán, C.; Marugán, J. Synergistic and antagonistic effects in the photoelectrocatalytic disinfection of water with TiO₂ supported on activated carbon as a bipolar electrode in a novel 3D photoelectrochemical reactor. *Sep. Purif. Technol.* **2020**, *247*, 117002. [[CrossRef](#)]
124. Ahmadian, A.; Ehn, M.; Hober, S. Pyrosequencing: History, biochemistry and future. *Clin. Chim. Acta* **2006**, *363*, 83–94. [[CrossRef](#)]
125. Alp, E.; Imamoğlu, R.; Savacı, U.; Turan, S.; Kazmanlı, M.; Genç, A. Plasmon-enhanced photocatalytic and antibacterial activity of gold nanoparticles-decorated hematite nanostructures. *J. Alloy. Compd.* **2020**, *852*, 157021. [[CrossRef](#)]
126. Fittipaldi, M.; Nocker, A.; Codony, F. Progress in understanding preferential detection of live cells using viability dyes in combination with DNA amplification. *J. Microbiol. Methods* **2012**, *91*, 276–289. [[CrossRef](#)] [[PubMed](#)]
127. Bauer, A. Antibiotic susceptibility testing by a standardized single disc method. *Am. J. Clin. Pathol.* **1966**, *45*, 149–158. [[CrossRef](#)]
128. Kayani, Z.N.; Abbas, E.; Saddiqe, Z.; Riaz, S.; Naseem, S. Photocatalytic, antibacterial, optical and magnetic properties of Fe-doped ZnO nano-particles prepared by sol-gel. *Mater. Sci. Semicond. Process.* **2018**, *88*, 109–119. [[CrossRef](#)]
129. Sunada, K.; Kikuchi, Y.; Hashimoto, K.; Fujishima, A. Bactericidal and Detoxification Effects of TiO₂Thin Film Photocatalysts. *Environ. Sci. Technol.* **1998**, *32*, 726–728. [[CrossRef](#)]
130. Fujishima, A.; Rao, T.N.; Tryk, D.A. Titanium dioxide photocatalysis. *J. Photochem. Photobiol. C Photochem. Rev.* **2000**, *1*, 1–21. [[CrossRef](#)]
131. Montenegro-Ayo, R.; Barrios, A.C.; Mondal, I.; Bhagat, K.; Morales-Gomero, J.C.; Abbaszadegan, M.; Westerhoff, P.; Perreault, F.; Garcia-Segura, S. Portable point-of-use photoelectrocatalytic device provides rapid water disinfection. *Sci. Total. Environ.* **2020**, *737*, 140044. [[CrossRef](#)]
132. Kassahun, S.K.; Kiflie, Z.; Kim, H.; Gadisa, B.T. Effects of operational parameters on bacterial inactivation in Vis-LEDs illuminated N-doped TiO₂ based photoreactor. *J. Environ. Chem. Eng.* **2020**, *8*, 104374. [[CrossRef](#)]
133. Alrousan, D.M.; Dunlop, P.S.M.; McMurray, T.A.; Byrne, J.A. Photocatalytic inactivation of *E. coli* in surface water using immobilised nanoparticle TiO₂ films. *Water Res.* **2009**, *43*, 47–54. [[CrossRef](#)]
134. McMurray, T.; Byrne, J.A.; Dunlop, P.; Winkelman, J.; Eggins, B.; McAdams, E. Intrinsic kinetics of photocatalytic oxidation of formic and oxalic acid on immobilised TiO₂ films. *Appl. Catal. A Gen.* **2004**, *262*, 105–110. [[CrossRef](#)]
135. Kubista, M.; Andrade, J.M.; Bengtsson, M.; Forootan, A.; Jonák, J.; Lind, K.; Sindelka, R.; Sjöback, R.; Sjögreen, B.; Strömbom, L.; et al. The real-time polymerase chain reaction. *Mol. Asp. Med.* **2006**, *27*, 95–125. [[CrossRef](#)] [[PubMed](#)]
136. Unluturk, S.; Atılgan, M.R.; Baysal, A.H.; Unluturk, M.S. Modeling inactivation kinetics of liquid egg white exposed to UV-C irradiation. *Int. J. Food Microbiol.* **2010**, *142*, 341–347. [[CrossRef](#)] [[PubMed](#)]
137. Bialka, K.L.; Demirci, A.; Puri, V.M. Modeling the inactivation of *Escherichia coli* O157:H7 and *Salmonella enterica* on raspberries and strawberries resulting from exposure to ozone or pulsed UV-light. *J. Food Eng.* **2008**, *85*, 444–449. [[CrossRef](#)]
138. van Boekel, M.A. On the use of the Weibull model to describe thermal inactivation of microbial vegetative cells. *Int. J. Food Microbiol.* **2002**, *74*, 139–159. [[CrossRef](#)]
139. Moter, A.; Göbel, U.B. Fluorescence in situ hybridization (FISH) for direct visualization of microorganisms. *J. Microbiol. Methods* **2000**, *41*, 85–112. [[CrossRef](#)]
140. Girones, R.; Ferrús, M.A.; Alonso, J.L.; Rodriguez-Manzano, J.; Calgua, B.; Corrêa, A.D.A.; Hundesa, A.; Carratala, A.; Bofill-Mas, S. Molecular detection of pathogens in water—The pros and cons of molecular techniques. *Water Res.* **2010**, *44*, 4325–4339. [[CrossRef](#)]
141. Law, J.W.-F.; Ab Mutalib, N.-S.; Chan, K.-G.; Lee, L.-H. Rapid methods for the detection of foodborne bacterial pathogens: Principles, applications, advantages and limitations. *Front. Microbiol.* **2015**, *5*, 770. [[CrossRef](#)]
142. Paton, A.W.; Paton, J.C. Detection and Characterization of Shiga Toxigenic *Escherichia coli* by Using Multiplex PCR Assays forstx 1, stx 2, eaeA, Enterohemorrhagic *E. coli* hlyA, rfb O111, and rfb O157. *J. Clin. Microbiol.* **1998**, *36*, 598–602. [[CrossRef](#)]

143. Omar, K.B.; Barnard, T.G. Detection of diarrhoeagenic *Escherichia coli* in clinical and environmental water sources in South Africa using single-step 11-gene m-PCR. *World J. Microbiol. Biotechnol.* **2014**, *30*, 2663–2671. [[CrossRef](#)]
144. Omiccioli, E.; Amagliani, G.; Brandi, G.; Magnani, M. A new platform for Real-Time PCR detection of *Salmonella* spp., *Listeria monocytogenes* and *Escherichia coli* O157 in milk. *Food Microbiol.* **2009**, *26*, 615–622. [[CrossRef](#)]
145. Ma, J.; Ibekwe, A.M.; Yang, C.-H.; Crowley, D.E. Influence of bacterial communities based on 454-pyrosequencing on the survival of *Escherichia coli* O157:H7 in soils. *FEMS Microbiol. Ecol.* **2013**, *84*, 542–554. [[CrossRef](#)] [[PubMed](#)]
146. Siqueira, J.F.; Fouad, A.F.; Rôças, I.N. Pyrosequencing as a tool for better understanding of human microbiomes. *J. Oral. Microbiol.* **2012**, *4*. [[CrossRef](#)] [[PubMed](#)]
147. Stender, H.; Oliveira, K.; Rigby, S.; Bargoot, F.; Coull, J. Rapid detection, identification, and enumeration of *Escherichia coli* by fluorescence in situ hybridization using an array scanner. *J. Microbiol. Methods* **2001**, *45*, 31–39. [[CrossRef](#)]
148. Zhu, L.; Li, S.; Shao, X.; Feng, Y.; Xie, P.; Luo, Y.; Huang, K.; Xu, W. Colorimetric detection and typing of *E. coli* lipopolysaccharides based on a dual aptamer-functionalized gold nanoparticle probe. *Microchim. Acta* **2019**, *186*, 111. [[CrossRef](#)]
149. Pandey, C.M.; Tiwari, I.; Singh, V.N.; Sood, K.; Gajjala, S.; Malhotra, B.D. Highly sensitive electrochemical immunosensor based on graphene-wrapped copper oxide-cysteine hierarchical structure for detection of pathogenic bacteria. *Sens. Actuat. B Chem.* **2017**, *238*, 1060–1069. [[CrossRef](#)]
150. Rainina, E.; Efremenco, E.; Varfolomeyev, S.; Simonian, A.; Wild, J. The development of a new biosensor based on recombinant *E. coli* for the direct detection of organophosphorus neurotoxins. *Biosens. Bioelectron.* **1996**, *11*, 991–1000. [[CrossRef](#)]
151. Wang, L.; Liu, Q.; Hu, Z.; Zhang, Y.; Wu, C.; Yang, M.; Wang, P. A novel electrochemical biosensor based on dynamic polymerase-extending hybridization for *E. coli* O157:H7 DNA detection. *Talanta* **2009**, *78*, 647–652. [[CrossRef](#)]
152. Singh, A.; Poshtiban, S.; Evoy, S. Recent Advances in Bacteriophage Based Biosensors for Food-Borne Pathogen Detection. *Sensors* **2013**, *13*, 1763–1786. [[CrossRef](#)]